Evaluation of cleaning conditions for polymeric ultrafiltration membranes after black liquor filtration

DEPARTMENT OF PROCESS AND LIFE SCIENCE ENGINEERING| LUND UNIVERSITY

KATERYNA SVYRHUN| MASTER THESIS 2026

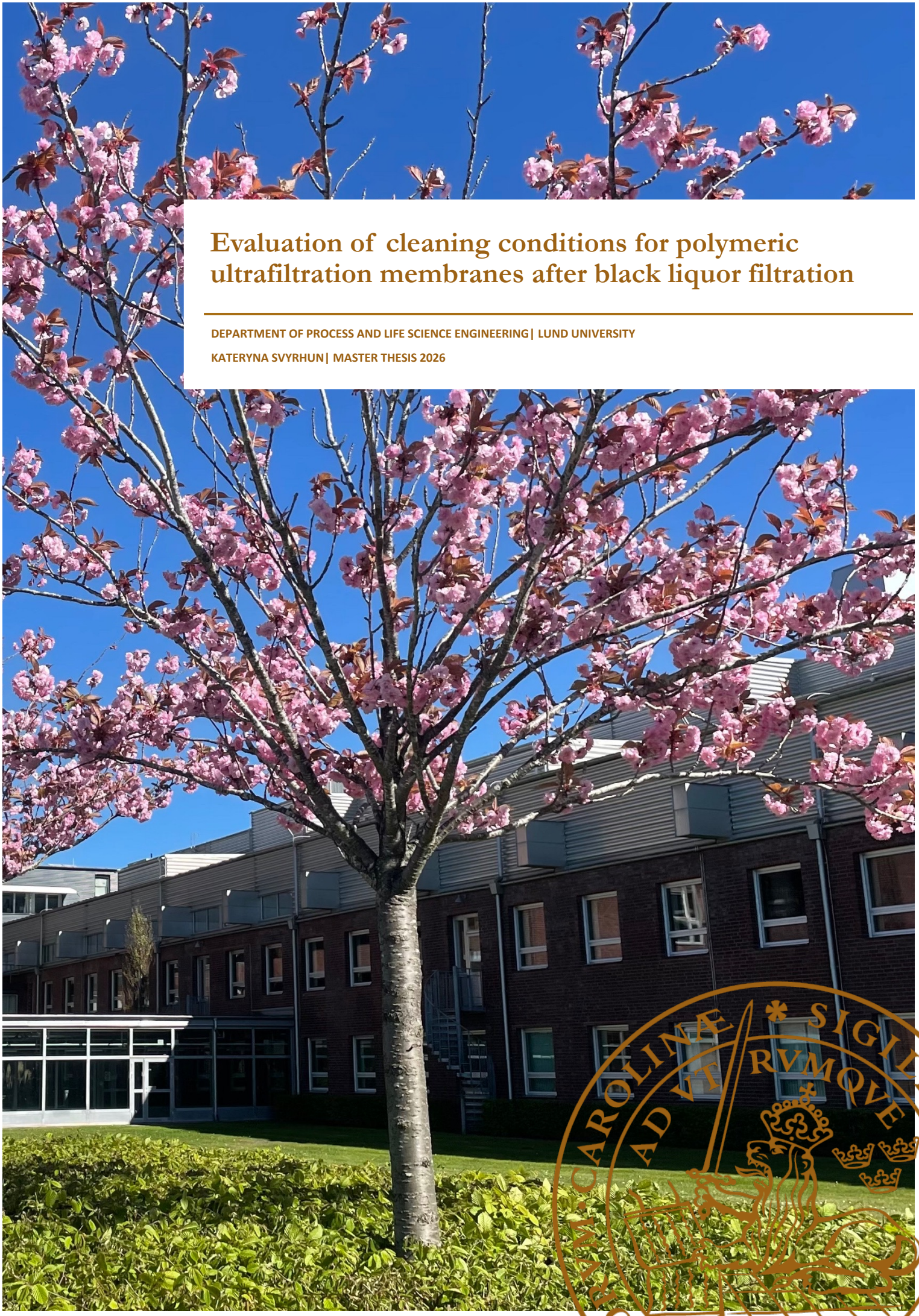

Evaluation of cleaning conditions for polymeric ultrafiltration membranes after black liquor filtration

by

Kateryna Svyrhun

Division of Chemical Engineering
Department of Process and Life Science Engineering
Lund University

May 2026

Supervisor: **Mariona Battestini Vives**
Examiner: **Professor Frank Lipnizki**

Postal address
Box 124
SE-221 00 Lund, Sweden
Web address
http://www.ple.lth.se

Visiting address
Kemicentrum
Naturvetarvägen 22
223 62 Lund, Sweden

Telephone
+46 46-222 82 85
+46 46-222 00 00

Funded by the European Union

Acknowledgement

The author thanks the European Commission – Education, Audiovisual and Culture Executive Agency (EACEA) for the Erasmus Mundus scholarship under the program: Master in Membrane Engineering for Sustainable Development (MESD), Project number: 101081874, Call: ERASMUS-EDU-2022-PEX-EMJM-MOB.

EU Funding Statement

Funded by the European Union. Views and opinions expressed are however those of the author(s) only and do not necessarily reflect those of the European Union or EACEA. Neither the European Union nor the granting authority can be held responsible for them.

MESD Partner Institutions

Preface

This thesis work was carried out at Kemicentrum, Faculty of Engineering, Lund University, Sweden. The experimental work was performed at Pilot Hall during the Spring 2026 semester. I am grateful for the opportunity to conduct this project in such a supportive academic and laboratory environment.

My sincere gratitude goes to my supervisor, Mariona Battestini Vives, for her continuous guidance, support, and encouragement throughout this thesis. The experimental work involved long and intensive weeks in the laboratory, and there were several moments when the process felt overwhelming. Mariona's patience, kindness, and willingness to help made a significant difference during this project. I am very thankful for her supervision and for always making me feel that I could ask questions when I needed support.

I would also like to thank Frank Lipnizki for his teaching and contribution to the membrane engineering field. It has been a privilege to learn from him during my studies. I would also like to thank the staff and colleagues at Kemicentrum for their assistance, practical help, and welcoming atmosphere during the experimental work.

I am incredibly grateful for the opportunity to study at Lund University and to be part of the Erasmus Mundus MESD programme. Over these two years, I had the chance to study in different countries, meet people from many backgrounds, and learn in a truly international environment. This experience has become one of the most valuable parts of my academic and personal journey.

Finally, I would like to thank my family for their endless love, encouragement, and support throughout these two years. This master's programme was not always easy, but their support helped me continue moving forward.

Use of Generative AI Tools and Language Support Tools

Parts of this thesis were prepared with the assistance of generative AI, AI-assisted language support tools, and visual design tools, including ChatGPT, Claude, Grammarly, DeepL, and Canva.

ChatGPT and Claude were used to support language correction, grammar polishing, improving readability, reformulating text, and structuring selected sections based on the author's experimental work, notes, results, and literature sources. Grammarly and DeepL were used for English language support, including grammar correction, wording improvement, readability polishing, and translation assistance where needed.

ChatGPT and Canva were used to assist in the preparation and visual formatting of Figure 2.3, Figure 2.4, and the experimental workflow figure (Figure 3.3). The figures were based on the author's interpretation of the literature and experimental procedure and were reviewed by the author.

All AI-assisted text and visual material were reviewed, edited, and verified by the author. The author takes full responsibility for the final content of the thesis, including the experimental data, interpretation of results, references, figures, and conclusions.

Popular Scientific Summary

Why is membrane cleaning important in the pulp and paper industry?

The pulp and paper industry generates large process streams containing organic and inorganic compounds. One example is black liquor, a by-product formed during wood processing. Instead of treating such streams only as waste, membrane filtration can help recover valuable compounds and produce cleaner water streams for reuse.

However, membrane fouling is one of the main challenges in this process. During filtration, particles and organic compounds can accumulate on the membrane surface or inside the pores. This reduces flux and limits long-term membrane operation. Therefore, effective cleaning is needed to restore membrane performance.

What was investigated in this thesis?

This thesis investigated the chemical cleaning of a polymeric ultrafiltration membrane after black liquor filtration. The membrane was first fouled with black liquor, and then different cleaning conditions were tested to see how well the membrane performance could be recovered.

Three cleaning parameters were studied: cleaning temperature, cleaning solution concentration, and cleaning time. Eight cleaning experiments were performed using a Design of Experiments approach, followed by one validation experiment under the condition suggested by the model.

The membrane was also analysed before fouling, after fouling, and after cleaning using surface characterisation methods. These analyses were used to evaluate visible and measurable changes on the membrane surface and structure.

What were the main findings?

Black liquor filtration caused a gradual decrease in membrane flux, confirming that fouling developed during the experiment. Chemical cleaning recovered part of the membrane performance, but the recovery depended on the cleaning conditions used.

Among the tested conditions, the best recovery was obtained at the highest tested temperature and cleaning-agent concentration, corresponding to 50 °C and 1 wt.% Ultrasil 110. Cleaning time had a smaller effect within the tested range. The validation experiment gave a slightly higher flux recovery than the best result from the original experimental design, but the model should be interpreted carefully because only a limited number of experiments was performed.

Surface analysis showed local deposits on the fouled membrane. After cleaning, part of this material was removed, although the membrane surface was not fully restored to its initial condition. Overall, the study showed that chemical cleaning can improve membrane performance after black liquor fouling, but more experiments are needed to confirm the observed trends.

Summary

This thesis investigated the chemical cleaning of a polymeric ultrafiltration membrane after black liquor filtration. The main objective was to evaluate how cleaning temperature, cleaning-agent concentration, and cleaning time affected flux recovery after cleaning.

Black liquor filtration caused a gradual decline in permeate flux during the 25 h fouling experiment, confirming that fouling developed on the membrane. After fouling, eight cleaning experiments were performed using a full factorial Design of Experiments approach. The fouling factor was not identical in all experiments, which means that the initial degree of fouling varied between membrane samples and should be considered when interpreting the cleaning results.

The cleaning experiments showed that the highest flux recovery was obtained using Ultrasil 110 at 50 °C and 1 wt.%. The highest measured recovery in the experimental design was achieved after 30 min of cleaning, while the model suggested 60 min as the most favourable condition within the investigated range. Therefore, the validation experiment was performed at 50 °C, 1 wt.% Ultrasil 110, and 60 min. The validation experiment resulted in a flux recovery of 76.43%, which was slightly higher than the best result obtained in the original experimental design. The model should be treated as a screening tool rather than a strong predictive model because of the limited dataset and the absence of statistically significant effects.

Membrane characterisation was performed using scanning electron microscopy with energy-dispersive X-ray spectroscopy (SEM–EDS), atomic force microscopy (AFM), and Brunauer–Emmett–Teller (BET) nitrogen adsorption–desorption analysis. SEM–EDS and AFM showed that black liquor fouling caused local surface deposits and increased surface heterogeneity. After cleaning, the surface appeared partly restored, although some deposits and irregularities remained. BET analysis showed only small differences between the conditioned, fouled, and cleaned samples, suggesting that major changes in the nitrogen-accessible pore structure were not detected.

Overall, the results showed that cleaning temperature and cleaning-agent concentration were the most important parameters within the tested range, while cleaning time had a weaker effect. Chemical cleaning improved membrane performance after black liquor fouling, but additional experiments with repetitions and more factor levels would be needed to confirm the trends and improve reliability of the model.

Table of Contents

1. Introduction

Due to increasing environmental concerns and the growing demand for sustainable industrial processes, there is a strong interest in replacing fossil-based resources with renewable biomass-derived alternatives [1]. In this transition, lignocellulosic biorefineries play an important role by converting biomass into valuable products, chemicals, and energy [2]. The pulp and paper industry is one of the largest lignocellulosic biorefinery sectors, as wood components can be separated and further utilised instead of being treated as waste streams [3].

Wood mainly consists of cellulose, hemicelluloses, and lignin. During kraft pulping, cellulose fibres are separated for paper production, while the remaining lignin-rich stream forms kraft black liquor (KBL). Traditionally, black liquor is combusted for energy and chemical recovery. However, lignin is a valuable compound that can be further utilised to produce biofuels, resins, adhesives, carbon materials, and other bio-based chemicals [4, 5]. Recovering lignin from black liquor could contribute to resource efficiency and the development of sustainable industrial processes.

Membrane filtration has gained increasing attention in lignocellulosic biorefineries due to its relatively low energy demand, moderate operating conditions, and high separation efficiency [6]. Pressure-driven membrane processes such as ultrafiltration (UF) and nanofiltration (NF) have been widely used for lignin concentration and fractionation from black liquor streams [7].

Despite the promising potential of membrane processes, membrane fouling remains one of the major limitations during black liquor filtration [8, 9]. Fouling leads to flux decline, reduced separation performance, and increased operational costs. Effective membrane cleaning is therefore essential to restore membrane performance. Several studies have investigated chemical cleaning strategies for membrane systems, but the optimisation of cleaning conditions for black liquor filtration remains an important research area [10, 11].

In this thesis, the cleaning of a polymeric ultrafiltration membrane used for black liquor filtration was investigated. The study focused on evaluating how different cleaning parameters influenced membrane performance and flux recovery after fouling. A Design of Experiments (DOE) approach was applied to study the effects of cleaning temperature, cleaning time, and cleaning solution concentration.

1.1 Aim of the thesis

The main aim of this thesis was to investigate the cleaning procedure of a polymeric ultrafiltration membrane used for black liquor filtration. The study focused on understanding how different cleaning conditions influence flux recovery and membrane performance after fouling.

The specific objectives of the thesis were:

1. To investigate the influence of cleaning temperature, cleaning time, and cleaning solution concentration on membrane cleaning efficiency.
2. To identify suitable cleaning conditions using a DOE approach.
3. To validate the selected cleaning parameters.
4. To analyse membrane surface changes before and after fouling, and after cleaning using membrane characterisation analysis.

2. Background

2.1 Membrane Filtration

Membrane filtration is a physical separation process that uses a membrane to remove particles, microorganisms, and solutes from liquids or gases [12]. The membrane acts as a thin, semi-permeable barrier that allows certain components of a mixture to pass through, while larger or unwanted components are retained. This divides the feed stream into two streams: the permeate, which passes through the membrane, and the retentate, which contains the rejected components. Separation can be based on differences in particle size, molecular weight, charge, or affinity between the membrane and the separated compounds. Membrane processes are driven by a difference in chemical potential across the membrane, which can be created by pressure, concentration, electrical potential, or temperature gradients [12, 13].

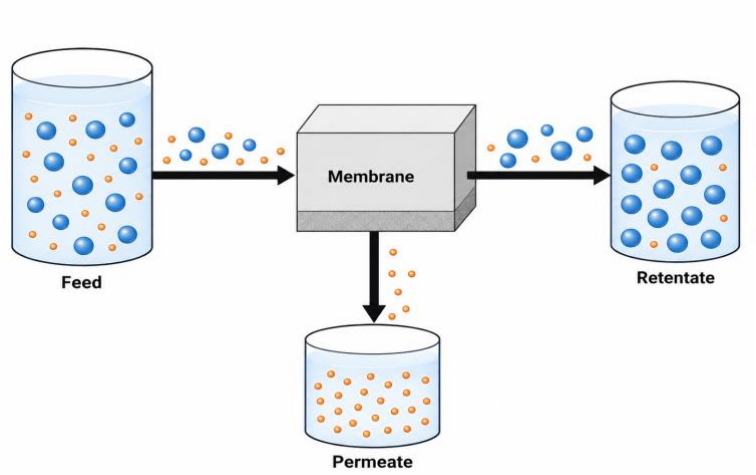

Figure 2.1. Schematic illustration of membrane filtration. Adapted from [14].

2.1.1 Pressure-driven membrane processes

Pressure-driven membrane filtration is commonly used in many industrial applications, particularly for the separation and purification of liquid streams. In pressure-driven membrane processes, pressure is used to force the feed solution through the membrane, which allows selective separation of components according to membrane characteristics [13]. Compared to conventional separation techniques such as distillation or solvent extraction, pressure-driven membrane processes do not require phase changes or the addition of chemicals to the feed stream [13]. They can be operated at relatively mild temperatures, which makes them suitable for heat-sensitive materials, including food and bioprocessing streams [13].

2.1.2 Classification of pressure-driven membrane processes

Pressure-driven membrane processes are commonly divided into microfiltration (MF), ultrafiltration (UF), nanofiltration (NF), and reverse osmosis (RO). These processes differ in the size of compounds they retain, their separation mechanism, and the pressure usually required for operation (Table 2.1). In general, the separation range becomes smaller from MF to RO: MF retains suspended particles and microorganisms, UF retains colloids and macromolecules, NF retains small organic compounds and multivalent ions, and RO is mainly used for desalination and removal of low-molecular-weight dissolved species [13, 16].

Table 2.1. Overview of pressure-driven membrane filtration processes. Adapted from [13] and [15].

Process	Typical pressure (bar)	Pore size / MWCO	Separation mechanism	Typical retained compound
Microfiltration	1–2	0.1–10 µm	Sieving / size exclusion	Removal of suspended solids and bacteria
Ultrafiltration	1–10	1–200 kDa	Size exclusion	Separation of proteins, colloids and macromolecules
Nanofiltration	5–40	300–1000 Da	Size exclusion + charge effects	Removal of divalent ions and small organics
Reverse osmosis	15–150	<200 Da	Solution–diffusion	Desalination and water purification

Pressure-driven membrane processes are usually operated in two modes: dead-end and crossflow. In dead-end filtration, the feed flows perpendicular to the membrane surface, causing retained particles to accumulate on the membrane surface. As filtration proceeds, these deposits form a cake layer that increases filtration resistance and may reduce membrane performance. In crossflow filtration, the feed flows parallel to the membrane surface. The tangential flow helps to limit the accumulation of foulants by continuously sweeping part of the deposited material away from the membrane surface [12].

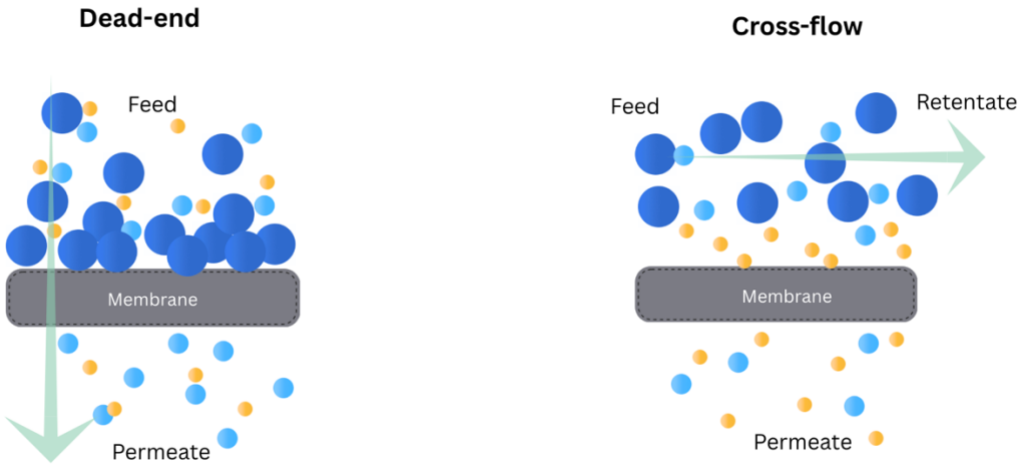

Figure 2.2. Schematic illustration of dead-end and cross-flow filtration modes. Adapted from [13].

2.1.3 Permeate Flux and Transmembrane Pressure

Transmembrane pressure (TMP) is the pressure difference across the membrane and represents the driving force for pressure-driven filtration. It is defined as the difference between the pressure on the feed side and the pressure on the permeate side of the membrane [13]. For a crossflow system, TMP is calculated as the average of the feed inlet (P_{feed}) and retentate outlet pressures ($P_{retentate}$) minus the permeate-side pressure ($P_{permeate}$) [17].

The transmembrane pressure was calculated according to Equation (1):

$$TMP = \frac{P_{feed} + P_{retentate}}{2} - P_{permeate} \quad (1)$$

Permeate flux, *J*, describes the volume of permeate passing through a unit membrane area per unit time. It is commonly expressed in L m^{-2} h^{-1}. For pure water filtration through a clean membrane, flux can be described by Darcy's law, where *J* is proportional to *TMP* and inversely proportional to the dynamic viscosity of the permeate (μ) and the intrinsic membrane resistance (R_m) [17]:

$$J = \frac{TMP}{\mu \cdot R_m} \quad (2)$$

In this work, pure water flux (*PWF*) was used to evaluate changes in membrane permeability before fouling, after fouling, and after cleaning. The pure water flux measured before fouling was denoted as PWF_1, the pure water flux measured after fouling as PWF_2, and the pure water flux measured after cleaning as PWF_3. The fouling factor (*FF*), which describes the relative decrease in pure water flux caused by fouling, and flux recovery (*FR*), which describes the extent to which the initial pure water flux was restored after cleaning, were calculated according to Equations (3) and (4), respectively [11].

$$FF\ (\%) = \frac{PWF_1 - PWF_2}{PWF_1} \cdot 100 \quad (3)$$

$$FR\ (\%) = \frac{PWF_3}{PWF_1} \cdot 100 \quad (4)$$

A higher fouling factor indicates a stronger decrease in membrane permeability after fouling. Higher flux recovery indicates more effective restoration of membrane permeability after cleaning.

2.1.4 Concentration polarization

Concentration polarization is a common phenomenon in membrane filtration in which rejected solutes accumulate near the membrane surface, resulting in a higher solute concentration at the membrane surface than in the bulk feed solution [13, 17].

Concentration polarization can be described using the film model presented in Equation (5):

$$J = k \cdot ln\left[\frac{C_m - C_p}{C_b - C_p}\right] \quad (5)$$

where:

J – permeate flux (L m^{-2} h^{-1})
k – mass transfer coefficient (m s^{-1})
C_m – solute concentration at the membrane surface (kg m^{-3})
C_p – solute concentration in the permeate (kg m^{-3})
C_b – bulk solute concentration in the feed (kg m^{-3})

Unlike membrane fouling, concentration polarization is generally reversible and disappears when filtration stops. However, the increased solute concentration near the membrane surface

can promote gel formation, precipitation, and adsorption, which may eventually lead to membrane fouling [17].

2.1.5 Critical and Limiting Flux

Limiting flux refers to the maximum permeate flux that can be sustained under given operating conditions. As TMP increases, solutes accumulate near the membrane surface, increasing hydraulic resistance and limiting the flux improvement obtained from additional pressure increases. Eventually, the flux approaches a plateau, where further increase in TMP produces little or no increase in permeate flux [13].

Critical flux describes the flux below which fouling remains limited [18]. It can be represented in two forms. In the strong form, the critical flux is the point where the flux of a particle-containing feed first begins to deviate from the pure water flux line. In the weak form, the critical flux corresponds to the point where a deviation from a linear flux–TMP relationship is observed, indicating the beginning of fouling or concentration-polarisation effects. The relationship between pure water flux, critical flux in the strong and weak forms, and limiting flux is illustrated in Figure 2.3.

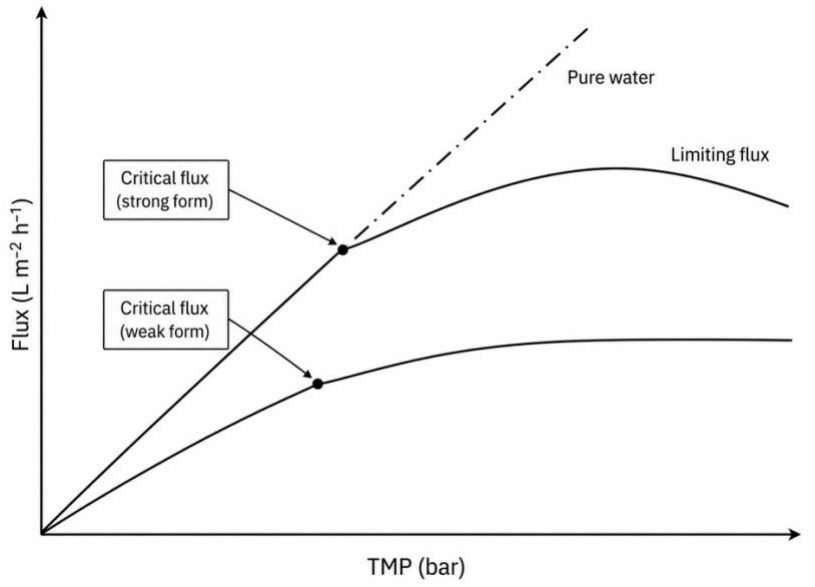

Figure 2.3. Schematic representation of pure water flux, limiting flux, and critical flux. Created by the author with the assistance of generative AI, based on Battestini Vives [10] and Rudolph [19].

These concepts are important in membrane process design because operation above the critical or limiting flux may accelerate fouling and increase cleaning requirements.

2.2 Membrane Fouling and Cleaning

2.2.1 Fouling Mechanisms

Membrane fouling is the undesirable accumulation of suspended or dissolved substances on the membrane surface or within its pores [17]. Fouling leads to a decline in membrane performance over time, typically causing a reduction in permeate flux, an increase in transmembrane pressure and may also change the separation performance of the membrane.

Fouling behaviour depends on both the feed composition and the operating conditions, such as membrane material, pressure, and temperature [17].

Several fouling mechanisms may occur during membrane filtration. These are commonly described as adsorption, pore blocking, and cake or gel layer formation. In practice, different fouling mechanisms often occur simultaneously [11, 13].

To describe the effect of fouling on permeate flux, the resistance-in-series model is commonly used [17]. In this approach, the total hydraulic resistance is divided into membrane resistance, reversible fouling resistance (R_{rev}), and irreversible fouling resistance (R_{irrev}), while $\Delta\Pi$ represents the osmotic pressure difference across the membrane.

The resistance-in-series model used to describe membrane fouling is shown in Equation (6):

$$J = \frac{TMP - \Delta\Pi}{\mu \cdot (R_m + R_{rev} + R_{irrev})} \quad (6)$$

2.2.2 Membrane fouling and cleaning

Membrane fouling is commonly divided into reversible and irreversible fouling depending on how easily the deposited material can be removed [17]. Reversible fouling is usually related to loosely attached foulants on the membrane surface and can often be reduced by physical or hydraulic cleaning methods, such as rinsing, flushing, or backwashing. In contrast, irreversible fouling occurs when foulants strongly attach to the membrane surface or enter membrane pores. This type of fouling is more difficult to remove and usually requires chemical cleaning [17, 20].

The choice of cleaning agent depends on the type of foulant present on the membrane. Alkaline cleaning solutions are commonly used for organic fouling, while acidic cleaning agents are mainly applied for inorganic scaling deposits [17]. Other cleaning strategies, including enzymatic or chelating agents, may also be used when specific foulants need to be targeted [11].

Cleaning efficiency is influenced by several operating parameters, including cleaning temperature, cleaning-agent concentration, cleaning time, and cleaning frequency [11]. These parameters must be selected carefully, since insufficient cleaning may leave deposits on the membrane surface, while overly harsh cleaning conditions can damage the membrane or reduce its lifetime.

2.3 Kraft Pulping Process and Black Liquor

2.3.1 Lignocellulosic Biomass and Lignin

Wood is a lignocellulosic material mainly composed of cellulose, hemicelluloses, and lignin. Cellulose forms the structural framework of the plant cell wall, while hemicelluloses and lignin surround the cellulose fibres and contribute to the mechanical strength of the biomass [21].

Lignin is a complex aromatic biopolymer and one of the most abundant natural polymers on Earth [9, 22]. In wood, lignin acts as a binding material between the cellulose fibres and provides rigidity to the plant structure. Due to lignin aromatic structure and high carbon content, lignin is considered a promising renewable source for fuels, chemicals, and functional materials [9, 22].

2.3.2 Kraft Pulping and Black Liquor Formation

Kraft pulping process is the most widely used chemical pulping method worldwide due to its ability to produce strong cellulose fibres and efficiently recover cooking chemicals [8, 21]. In this process, wood chips are treated with white liquor, which mainly consists of sodium hydroxide (NaOH) and sodium sulphide (Na_2S), at elevated temperature and pressure.

During kraft pulping, lignin and part of the hemicelluloses are dissolved from the wood matrix into the spent cooking liquor. After separation from the cellulose pulp, this spent liquor is referred to as black liquor.

The black liquor generated during pulping is concentrated and combusted in the chemical recovery cycle to recover energy and regenerate the cooking chemicals. However, the recovery boiler is often considered a bottleneck in kraft pulp mills, which has increased industrial interest in technologies for lignin separation before combustion [8, 23].

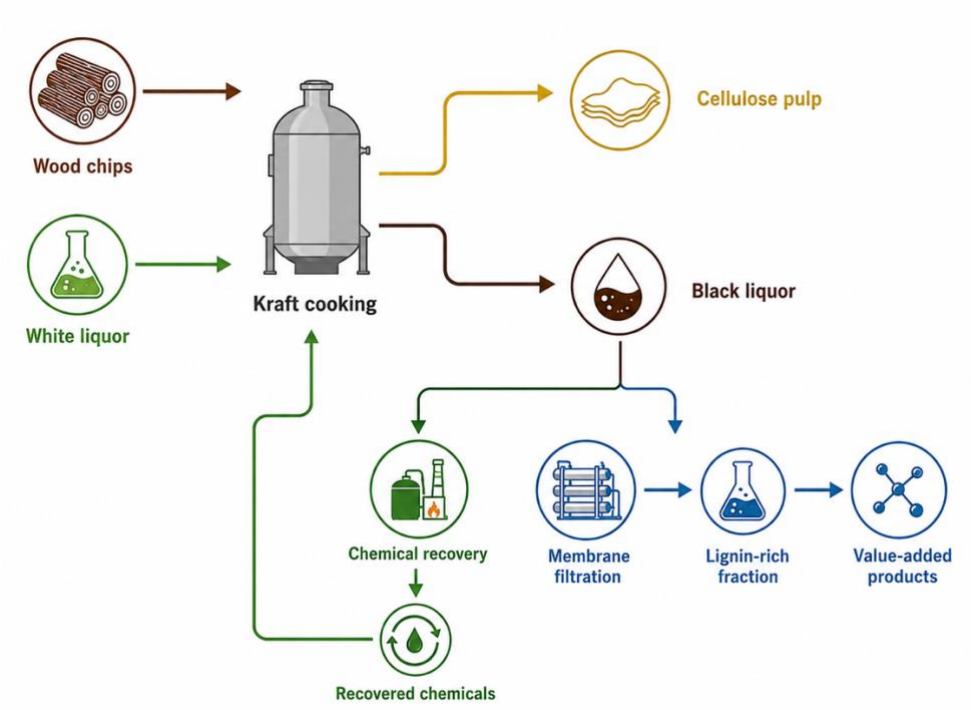

Figure 2.4. Simplified schematic of kraft pulping, black liquor formation, and recovery routes. Created by the author with the assistance of generative AI, based on [24].

2.3.3 Composition and Properties of Black Liquor

Black liquor is a highly alkaline solution containing dissolved organic and inorganic compounds originating from the kraft pulping process. The organic fraction mainly consists of lignin fragments together with degradation products from hemicelluloses and extractives, while the inorganic fraction contains residual chemicals based primarily on sodium compounds [8].

The composition and physicochemical properties of black liquor are important in membrane filtration applications because they influence viscosity, membrane stability, lignin aggregation behaviour, and fouling tendency. Black liquor typically has a pH above 12 and contains high concentrations of dissolved organic material, which can contribute to severe membrane fouling during ultrafiltration [8, 25].

2.3.4 Lignin Recovery by Membrane Filtration

Traditionally, kraft black liquor is combusted in the recovery boiler for energy generation and chemical recovery. However, recovering part of the lignin before combustion can reduce the load on the recovery boiler and create additional value streams from lignin-based products. The most established industrial lignin recovery method is acid precipitation, in which the pH of black liquor is lowered in order to decrease lignin solubility and induce precipitation. Commercial processes such as LignoBoost are based on this principle [22]. Membrane filtration, particularly UF, has also attracted significant research interest as an alternative or complementary approach for lignin recovery. Membrane-based recovery of lignin and hemicelluloses from pulp mill streams has also been discussed as a promising route for improving resource efficiency in pulp mill biorefineries [26]. Unlike acid precipitation, UF can be performed under the native alkaline conditions of black liquor and allows lignin to be fractionated according to molecular weight [25, 27, 28].

Several studies have demonstrated the feasibility of UF for kraft black liquor treatment using both ceramic and polymeric membranes [23, 29]. However, membrane fouling remains one of the main challenges limiting the long-term performance of black liquor ultrafiltration processes. The high concentration of dissolved organics, colloidal material, and inorganic species can lead to rapid flux decline and the formation of deposits on the membrane surface and inside the pores [8, 9].

Previous work on kraft black liquor nanofiltration has shown that membrane performance depends strongly on operating conditions and fouling behaviour, which makes cleaning and process optimisation important for long-term operation [10].

Operating conditions such as temperature, transmembrane pressure, and crossflow velocity strongly influence both filtration performance and fouling behaviour. Higher temperatures generally reduce viscosity and improve flux, while higher crossflow velocities help limit foulant accumulation at the membrane surface [8].

3. Materials and Methods

3.1 Membrane and filtration system

All experiments were performed using a GR80PP, which is flat-sheet ultrafiltration membrane supplied by Alfa Laval Nakskov A/S, Nakskov, Denmark. The membrane consists of a polyethersulfone active layer supported by a polypropylene structure and has a MWCO of 10 kDa according to the manufacturer's specifications [30].

Figure 3.1. Experimental membrane filtration setup (Alfa Laval TestUnit M20).

The membrane sheets were installed in a LabStak™ M20 plate-and-frame module connected to an Alfa Laval TestUnit M20 filtration system [31]. In this work, one membrane plate was used. Two flat-sheet membrane pieces were mounted on the plate, one on each side, giving a total effective area of 0.036 m². The system was operated in cross-flow mode and was equipped with a feed tank, circulation pump, heat exchanger connected to a water bath for temperature control, pressure gauges positioned before and after the membrane module, and a flowmeter for monitoring the circulation flow rate. During the experiments, the flow rate was kept at approximately 7 dm³/min.

3.2 Flux calculations

The effective membrane area used in the experiments was 36,000 mm² (0.036 m²). Permeate flux values (J) were calculated from the change in permeate mass (Δm) over a time (Δt) using the effective membrane area (A) and permeate density (ρ) according to (Equation 7).

$$J = \frac{\Delta m}{\rho \cdot A \cdot \Delta t} \tag{7}$$

The flux was calculated automatically by the LabVIEW 2019 data acquisition system from the mass recorded on the connected balance. The membrane area was entered into the software. The liquid density was assumed to be 1000 kg m⁻³, corresponding to the density of water. This assumption was applied consistently for all flux calculations.

3.3 Feed and permeate characterisation

3.3.1 Total solids, volatile solids, and ash content

The total solids, ash content, and volatile solids were determined for four black liquor-related samples: the initial feed black liquor, the initial permeate sample, the feed sample collected after overnight fouling experiments, and the permeate sample collected after overnight fouling experiments.

The procedure was adapted from the NREL Laboratory Analytical Procedure for ash determination in biomass, where dry oxidation at 575 °C is used to determine the inorganic ash fraction [32]. Although the original method was developed for biomass samples, the same principle was applied in this work to compare the amount of dry residue and inorganic material in the feed and permeate streams.

For each sample, 10 mL was transferred into a pre-weighed crucible. The crucibles were dried in an oven at 105 °C to remove water and then cooled in a desiccator before weighing. After weighing, the dried samples were heated in a furnace at 575 °C to combust the organic fraction and determine the remaining inorganic ash. The crucibles were cooled again in a desiccator before the final mass was recorded.

The total solids, ash content, and volatile solids were calculated using Equations (8) – (10):

$$TS\ (\%) = \frac{m_{105} - m_{crucible}}{m_{sample}} \times 100 \quad (8)$$

$$Ash\ (\%) = \frac{m_{575} - m_{crucible}}{m_{sample}} \times 100 \quad (9)$$

$$VS\ (\%) = TS - Ash \quad (10)$$

where m_{105} is the mass after drying at 105 °C, m_{575} is the mass after ignition at 575 °C, $m_{crucible}$ is the empty crucible mass, and m_{sample} is the sample mass.

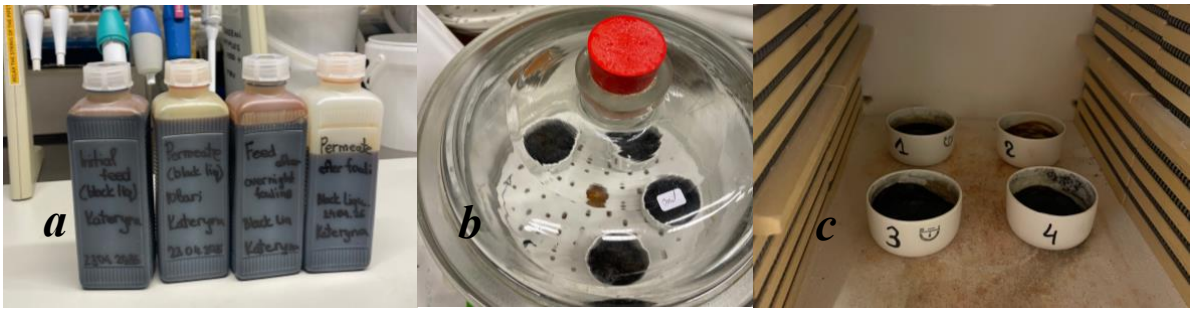

Figure 3.2. Experimental steps used for total solids, volatile solids, and ash content determination: (a) black liquor-related samples, (b) crucibles after thermal treatment and cooling in a desiccator, and (c) crucibles placed in the furnace.

3.3.2 UV–Vis analysis of lignin-related compounds

The total lignin content of the feed and permeate samples was determined by UV–Vis spectrophotometry. Due to the dark colour and high concentration of black liquor, the samples were diluted with NaOH solution before analysis. The absorbance of the diluted samples was measured at 280 nm using a Shimadzu UV-1800 UV–Vis spectrophotometer (Shimadzu Corporation, Kyoto, Japan).

The wavelength of 280 nm was selected because lignin contains aromatic structures that absorb strongly in this region. The dilution was adjusted so that the measured absorbance was within an appropriate range for UV–Vis analysis.

Lignin-related concentration was calculated from the absorbance measured at 280 nm using the Beer–Lambert relationship. The absorption coefficient used in this work was 23.6 g L^{-1} cm^{-1}. This value was calculated as a weighted coefficient from the softwood black liquor absorption coefficient of 24.6 g L^{-1} cm^{-1} reported by Arkell et al. [23] and the hardwood black liquor absorption coefficient of 21.1 g L^{-1} cm^{-1} reported by Jönsson et al. [25], assuming a 70% softwood and 30% hardwood contribution, following the assumption used by Battestini Vives et al. [16].

$$C_{lignin} = \frac{A_{280} \cdot DF}{\varepsilon \cdot l} \tag{11}$$

where A_{280} = absorbance at 280 nm, DF = dilution factor, ε = absorption coefficient, l = optical path length.

3.3.3 pH measurement

The pH of the black liquor feed solution was measured using a Hanna HI 8424 pH meter (Hanna Instruments, Woonsocket, Rhode Island, USA) equipped with a HI-11310 electrode. Before measurement, the pH meter was calibrated using standard buffer solutions at pH 7.01 and pH 4.01. The electrode was rinsed with deionized water between calibration and sample measurements.

3.4 Membrane fouling and cleaning experiments

The membrane fouling and cleaning experiments followed the same sequence for each tested cleaning condition. First, the membrane was conditioned and the initial pure water flux was measured. The system was then prepared under alkaline conditions before black liquor filtration. After fouling, the pure water flux was measured again, followed by chemical cleaning and a final pure water flux measurement. The full experimental workflow is shown in Figure 3.3.

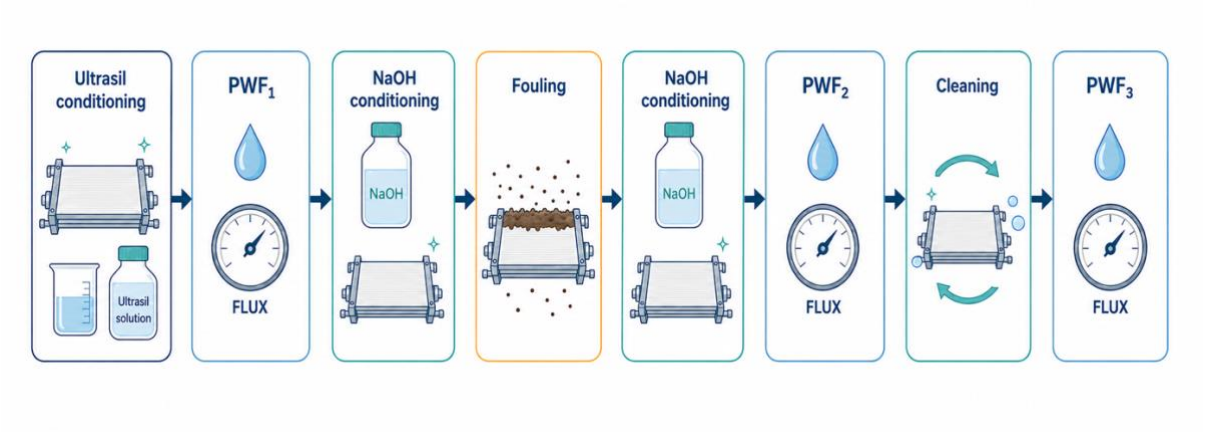

Figure 3.3. Workflow of the membrane fouling and cleaning experiments. The figure was prepared with the assistance of generative AI based on the author's experimental data and was reviewed by the author.

3.4.1 Conditioning

Membrane conditioning was carried out before each experiment using 5 litres of 1 wt.% Ultrasil 110 alkaline cleaning solution (Ecolab AB) prepared by dilution with deionized water. The solution was circulated through the system at 50 °C for 60 minutes.

This step was performed to remove residual foulants and impurities remaining from previous experiments and also to prepare the membrane before the filtration run. It also helped establish comparable starting conditions between experiments.

After conditioning, the membrane was rinsed with deionized water to remove the cleaning solution from the system. The initial pure water flux (PWF_1) was then measured according to the procedure described in Section 3.4.5 and used as the reference value for further analysis.

3.4.2 System preparation before black liquor filtration

Prior to introducing black liquor, the system was preconditioned using a sodium hydroxide (NaOH) solution (0.1 M). The solution was circulated through the system for approximately 30 minutes. This step allowed the system to adapt to alkaline conditions before black liquor filtration and helped avoid sudden pH changes during the experiment.

3.4.3 Membrane fouling

Membrane fouling was performed using 8 L of black liquor at a constant temperature of 50 °C. Both permeate and retentate were recirculated to the feed tank. The total fouling time was 25 hours. The transmembrane pressure profile was controlled as follows: the system was operated at 10 bar during the initial 4 hours, followed by operation at 4 bar during the main fouling period, and finally increased again to 10 bar during the last 2 hours. This pressure profile was selected to maintain stable fouling conditions and ensure safe overnight operation.

After completion of the fouling stage, the black liquor was removed from the system and collected in a designated waste container. Then, the membrane module and tubing were flushed by recirculating 0.1 M NaOH solution before the PWF_2 measurement. The pure water flux of the fouled membrane (PWF_2) was then measured.

3.4.4 Membrane cleaning

Chemical cleaning was performed using Ultrasil 110 by recirculating the cleaning solution through the membrane system. The cleaning conditions were selected according to the full factorial experimental design described in Section 3.5. The investigated parameters were cleaning temperature, cleaning agent (Ultrasil 110) concentration, and cleaning duration. During cleaning, the transmembrane pressure was maintained at approximately 2 bar.

After each cleaning step, the membrane was rinsed with deionized water until neutral pH was achieved. The pure water flux after cleaning (PWF_3) was then measured according to the procedure described in Section 3.4.5.

3.4.5 Pure water flux (PWF) measurements

Pure water flux (PWF) measurements were performed to evaluate membrane permeability before fouling, after fouling, and after chemical cleaning. Deionized water was used for all PWF measurements.

The measurements were carried out at three transmembrane pressures: 2, 4, and 6 bar. The water bath temperature was maintained at 30 °C. At each pressure, the permeate flux was recorded for 5 minutes using LabVIEW 2019. The mass signal from the connected balance was recorded every 10 seconds and used by the software to calculate flux.

The same procedure was applied for (PWF_1) after membrane conditioning, (PWF_2) after black liquor fouling, and (PWF_3) after chemical cleaning. These values were then used for the performance calculations described in Section 3.2.

3.5 Experimental design and validation

A DOE approach was used to plan the membrane cleaning experiments and evaluate the effect of cleaning conditions on flux recovery. The experimental design was prepared using JMP Student Edition 19 (SAS Institute Inc., Cary, NC, USA). A full factorial design was applied, meaning that every combination of the selected factor levels was tested. Flux recovery (%) was used as the response variable, while the fouling factor was calculated as supporting information to compare the extent of fouling before cleaning.

Table 3.1. Full factorial experimental matrix used for the membrane cleaning experiments.

Experiment	Temperature (°C)	Concentration (wt.%)	Time (min)
1	30	1	60
2	50	1	30
3	50	0.5	30
4	50	1	60
5	30	1	30
6	50	0.5	60
7	30	0.5	30
8	30	0.5	60

Three cleaning parameters were investigated: cleaning temperature, cleaning agent concentration, and cleaning duration. Each factor was tested at two levels: temperature at 30 and 50 °C, Ultrasil 110 concentration at 0.5 and 1 wt.%, and cleaning time at 30 and 60 minutes. This resulted in a 2^3 full factorial design with 8 cleaning experiments, as shown in Table 3.1.

The fouling procedure was kept the same before each cleaning experiment so that the effect of the cleaning conditions could be compared under consistent fouling conditions.

Flux recovery was selected as the main response variable because it describes how effectively membrane permeability was restored after cleaning. The fouling factor was calculated separately to describe the degree of flux decline caused by fouling before the cleaning step. After the eight cleaning experiments, a statistical model was developed in JMP and used to identify the model-predicted favourable cleaning condition within the investigated factor range. The validation experiment was therefore performed under the condition suggested by the model, rather than by simply repeating the experiment with the highest measured flux recovery.

3.6 Membrane surface characterisation

Membrane surface characterisation was performed to examine changes caused by black liquor fouling and chemical cleaning. Three membrane states were analysed: conditioned, fouled, and cleaned. The conditioned sample represented the membrane after the initial conditioning step, the fouled sample was taken after black liquor filtration, and the cleaned sample was taken after the validation cleaning experiment.

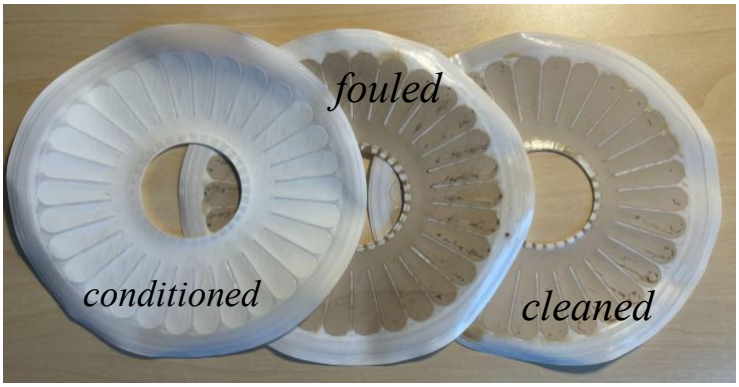

Figure 3.4. Membrane samples representing the three investigated membrane states.

Before analysis, the membrane samples were cut into smaller pieces suitable for each characterisation technique and handled carefully to avoid additional surface damage or contamination. Scanning electron microscopy with energy-dispersive X-ray spectroscopy (SEM–EDS), atomic force microscopy (AFM), and Brunauer–Emmett–Teller (BET) nitrogen adsorption/desorption analysis were used to evaluate surface morphology, elemental composition, surface roughness, surface area, and pore structure.

3.6.1 SEM–EDS

SEM–EDS was used to analyse the surface morphology and elemental composition of the conditioned, fouled, and cleaned membrane samples. Small pieces of each membrane sample were mounted on aluminium stubs using conductive carbon tape. Since the polymeric membrane material was non-conductive, the samples were sputter-coated with a 15 nm gold/palladium (Au/Pd) layer before analysis. The coating consisted of 80% Au and 20% Pd.

SEM–EDS analysis was performed using a JSM 6700F NT microscope (JEOL, Sollentuna, Sweden) equipped with an EDS detector from Oxford Instruments (Abingdon, UK). SEM images were collected at an accelerating voltage of 10 kV and at different magnifications, including ×5000 for comparison between membrane states. Elemental analysis was performed at an accelerating voltage of 20 kV. EDS spectra were collected from selected surface areas and analysed using AZtec software v2.3 (Oxford Instruments, Abingdon, UK).

3.6.2 Atomic force microscopy

Atomic force microscopy (AFM) was used to analyse membrane surface topography and roughness. Measurements were performed on conditioned, fouled, and cleaned membrane samples without additional coating. The samples were analysed using an XE-100 AFM instrument (Park Systems, Suwon, South Korea) in non-contact tapping mode. Scans were collected over an area of 5 × 5 μm at a scan rate of 0.25 Hz. The obtained images were analysed using software XEI version 1.8.0 from Park Systems, and the roughness parameters were calculated from the measured surface profiles.

3.6.3 Brunauer–Emmett–Teller analysis

Brunauer–Emmett–Teller (BET) nitrogen adsorption/desorption analysis was used to evaluate changes in the surface area and pore structure of the conditioned, fouled, and cleaned membrane samples. Before analysis, the samples were cut into smaller pieces and then dried in an oven at 30 °C for 30 minutes. The dried samples were then degassed under vacuum for 4 hours using a Smart VacPrep 067 degassing unit (Micromeritics Instrument Corporation, Norcross, Georgia, USA). This step was performed to remove residual moisture and physically adsorbed gases before nitrogen adsorption/desorption measurements.

The measurements were carried out using a Micromeritics 3Flex surface characterisation analyser (Micromeritics Instrument Corporation, Norcross, Georgia, USA). Nitrogen adsorption/desorption isotherms were used to determine the specific surface area by the BET method. Pore volume and pore size distribution were evaluated from the desorption branch using the Barrett–Joyner–Halenda (BJH) method.

4. Results and Discussion

4.1 Fouling development during black liquor filtration

The development of membrane fouling was first evaluated from the permeate flux measured during black liquor filtration. The average flux values recorded at stages of the 25-hour fouling experiment are shown in Figure 4.1.

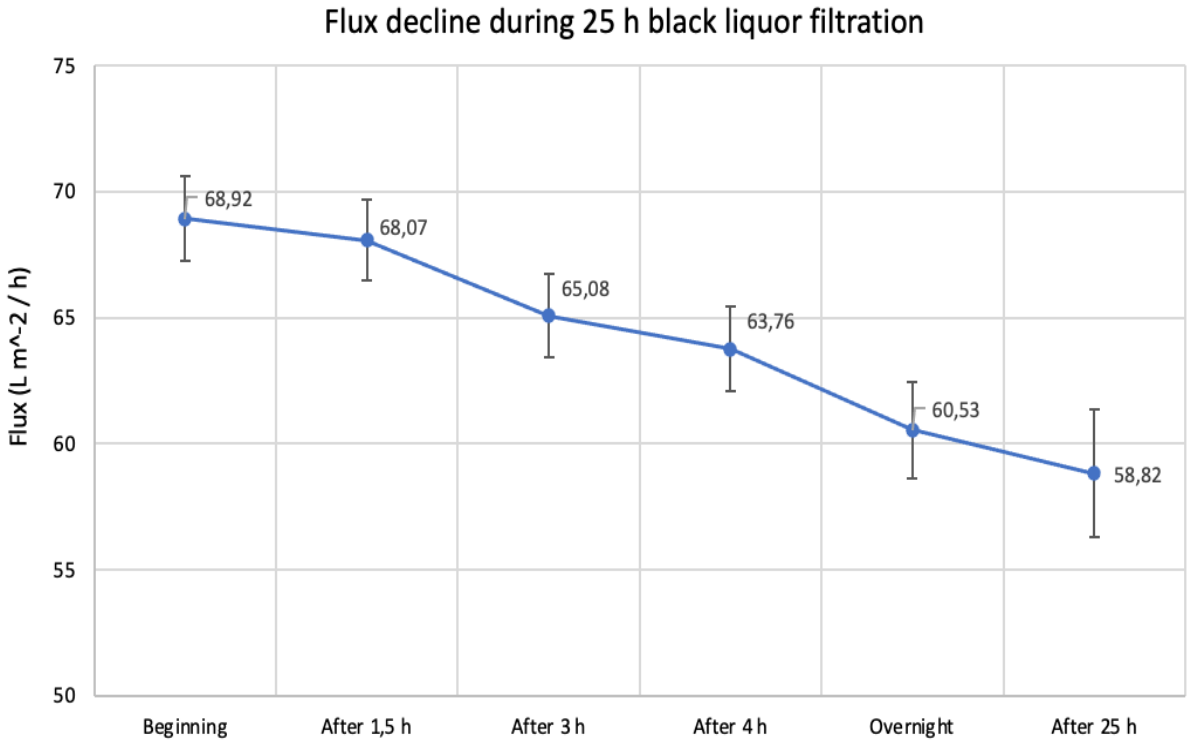

Figure 4.1. Flux decline during the 25-h black liquor fouling experiment. Error bars represent the standard deviation of the recorded flux values.

The permeate flux decreased from 68.92 L m^{-2} h^{-1} at the beginning of filtration to 58.82 L m^{-2} h^{-1} after 25 h. This corresponds to a flux decrease of approximately 14.7%. The decrease was gradual during the first hours of operation, with the flux decreasing to 63.76 L m^{-2} h^{-1} after 4 h. After overnight fouling, the flux was further reduced to 60.53 L m^{-2} h^{-1}. The final flux value remained lower than the initial value, showing that the membrane performance was affected by the fouling step before chemical cleaning.

The observed flux decline indicates that black liquor components were deposited on or within the membrane structure during filtration. This is expected for black liquor filtration, since lignin-related compounds, organic macromolecules, colloidal material, and inorganic salts can contribute to membrane fouling. This behaviour is consistent with the composition of kraft black liquor, which contains dissolved organic material, lignin-related compounds, and inorganic salts [8, 9].

4.2 Cleaning performance and DOE analysis

The cleaning performance results are summarized in Table 4.1. Flux recovery was used as the main response variable, while the fouling factor was included to show differences in the initial extent of fouling between experiments.

Table 4.1. Experimental conditions and membrane performance results.

Experiment	Temperature (°C)	Concentration (wt.%)	Time (min)	Fouling factor (%)	Flux recovery (%)
1	30	1	60	56.17	58.71
2	50	1	30	33.56	75.36
3	50	0.5	30	38.79	60.08
4	50	1	60	45.67	64.54
5	30	1	30	46.18	58.21
6	50	0.5	60	44.37	64.15
7	30	0.5	30	47.75	53.63
8	30	0.5	60	46.94	67.15

The fouling factor varied from 33.56% to 56.17% between the eight experiments (Table 4.1, Figure 4.2). This shows that the extent of fouling before cleaning was not identical in all experiments, although all membranes were fouled using the same black liquor filtration procedure. This variation should be considered when interpreting the flux recovery results, because differences in the initial fouling layer can affect how much flux can be recovered during cleaning.

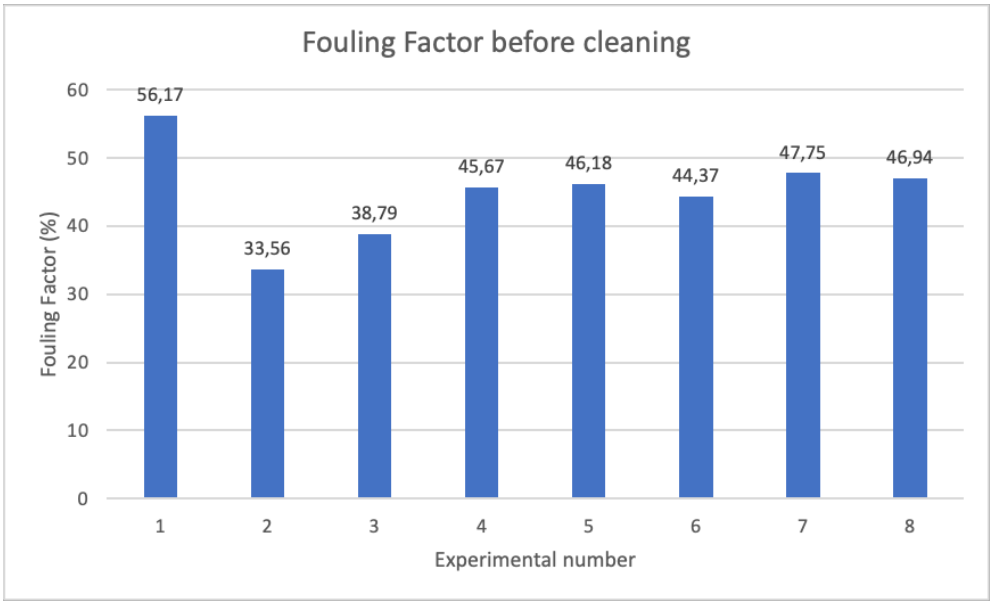

Figure 4.2. Fouling factor before chemical cleaning for the eight experiments.

The measured flux recovery varied from 53.63% to 75.36% (Table 4.1, Figure 4.3). The lowest flux recovery was obtained in Experiment 7, performed at 30 °C, 0.5 wt.% cleaning-agent concentration, and 30 min cleaning time. The highest measured flux recovery was obtained in

Experiment 2, performed at 50 °C, 1 wt.% cleaning-agent concentration, and 30 min cleaning time. This suggests that increasing the cleaning temperature from 30 to 50 °C and increasing the cleaning-agent concentration from 0.5 to 1 wt.% improved the recovery of membrane performance within the investigated range.

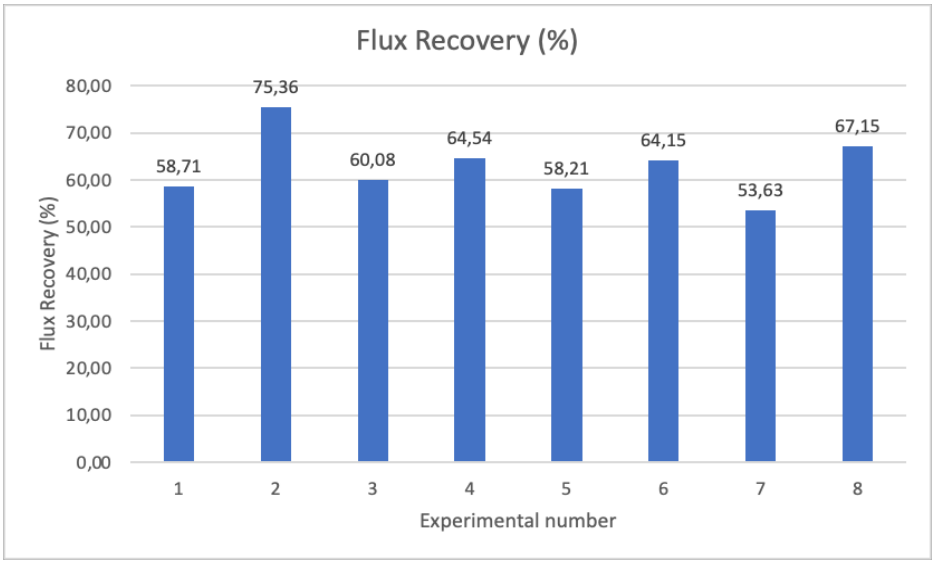

Figure 4.3. Flux recovery obtained after chemical cleaning for the eight experiments.

A statistical model was developed in JMP using flux recovery as the response and cleaning temperature, cleaning-agent concentration, and cleaning time as factors. The model was used to identify trends in the experimental dataset and to select conditions for the validation experiment. The obtained model is shown in Equation 12:

$$FR(\%) = 62.72875 + 3.30375 \cdot \left(\frac{T-40}{10}\right) + 1.47625 \cdot \left(\frac{C-0.75}{0.25}\right) + 0.90875 \cdot \left(\frac{t-45}{15}\right) \quad (12)$$

where *FR* is the predicted flux recovery, *T* is the cleaning temperature (°C), *C* is the cleaning-agent concentration (wt.%), and t is the cleaning time (min).

Table 4.2. Measured and predicted flux recovery values obtained from the JMP model.

Experiment	Flux recovery (%)	Predicted flux recovery (%)	Residual (%)
1	58.71	61.81	−3.10
2	75.36	66.60	8.76
3	60.08	63.65	−3.57
4	64.54	68.42	−3.88
5	58.21	59.99	−1.78
6	64.15	65.47	−1.32
7	53.63	57.04	−3.41
8	67.15	58.86	8.29

The residual represents the difference between the measured and predicted flux recovery value.

The predicted values from Table 4.2. did not fully match the measured flux recovery values. The residuals ranged from −3.88 to 8.76, showing that the model only partly described the experimental data. This agrees with the relatively low R^2 value of 0.36 and confirms that the model should be interpreted as a screening tool rather than as a reliable predictive model.

The prediction profiler shown in Figure 4.4 illustrates the estimated effect of cleaning temperature, Ultrasil 110 concentration, and cleaning time on the model response. In the upper row, the y-axis represents the predicted flux recovery (%), whereas the lower row shows the desirability function used in JMP for optimization. In this study, flux recovery was set to be maximized; therefore, higher desirability values correspond to more favourable operating conditions, while values closer to zero indicate less favourable conditions within the investigated range.

Among the tested factors, temperature showed the largest estimated effect on flux recovery, followed by cleaning-agent concentration and cleaning time. However, none of the factors was statistically significant at the 95% confidence level, with p-values of 0.256, 0.586, and 0.734, respectively. Therefore, the model should not be interpreted as a statistically significant predictive model, but rather as a screening tool for identifying practical trends in the dataset. The profiler predicted a flux recovery of 68.42% for the selected validation condition, with a desirability value of 0.66.

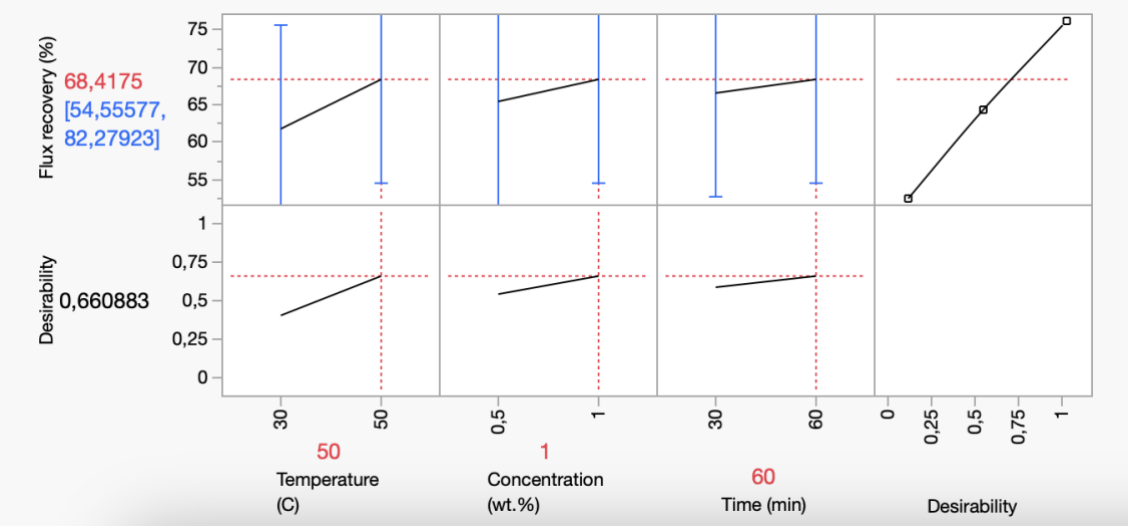

Figure 4.4. JMP prediction profiler showing the estimated effect of cleaning temperature, Ultrasil 110 concentration, and cleaning time on predicted flux recovery.

The prediction profiler was used to visualize the estimated effect of each cleaning factor on flux recovery while holding the other factors at the selected settings. In the upper panels, the y-axis represents the predicted flux recovery (%), whereas the lower panels show the desirability function used by JMP for optimization. Desirability is a dimensionless score ranging from 0 to 1, where values closer to 1 indicate more favourable conditions according to the selected optimization goal.

In this study, the goal was to maximize flux recovery; therefore, higher predicted flux recovery corresponds to higher desirability. The red dashed lines show the validation condition selected from the profiler: 50 °C, 1 wt.% Ultrasil 110, and 60 min.

Although the highest measured flux recovery among the eight experiments was obtained in Experiment 2 at 50 °C, 1 wt.% Ultrasil 110, and 30 min, this experiment also had the lowest fouling factor of 33.56%. Since the fouling factor varied between 33.56% and 56.17% across the experimental design, the initial degree of fouling was not identical before cleaning. Therefore, the high flux recovery in Experiment 2 may have been partly influenced by the lower initial fouling extent and should not be attributed only to the cleaning conditions.

The prediction profiler indicated 50 °C, 1 wt.% Ultrasil 110, and 60 min as the most favourable condition within the investigated factor range. These conditions were therefore selected for the validation experiment in order to test the model-predicted condition rather than simply repeat the run with the highest measured recovery.

This approach is consistent with the validation strategy used by Battestini Vives et al. [33], where the cleaning condition predicted by the model was experimentally tested instead of selecting only the experimental run with the highest observed response.

Using the JMP prediction formula, the predicted flux recovery for the validation condition was 68.42%, while the experimentally measured value was 76.43%. The validation result was higher than the model prediction and slightly higher than the highest measured recovery in the original experimental design. However, the model had limited predictive accuracy and none of the factors was statistically significant at the 95% confidence level. Therefore, the validation result should be interpreted as supporting a practical trend rather than confirming a statistically reliable optimum.

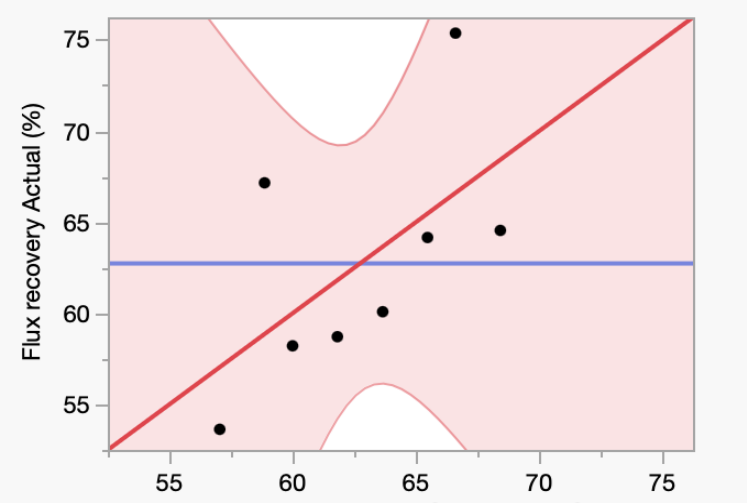

Figure 4.5. Actual by predicted plot for the DOE model of flux recovery.

The actual-by-predicted plot showed a weak fit between the measured and predicted flux recovery values. The model had an R^2 value of 0.36, meaning that approximately 36% of the variation in flux recovery was explained by the selected factors. The overall model p-value was 0.579, showing that the model was not statistically significant at the 95% confidence level. This limited model fit is most likely related to the small number of experiments, the absence of replicated runs, and possible differences in fouling layer formation before cleaning. For this reason, the model was used only to guide the selection of validation conditions and to identify trends, rather than to make strong quantitative predictions.

4.3 Feed and permeate characterisation

4.3.1 pH measurement

The measured pH value of the black liquor feed was 12.51, confirming the highly alkaline nature of the solution. This is consistent with kraft black liquor, which contains alkaline pulping chemicals and dissolved organic material from wood processing [8].

4.3.2 Total solids, ash content, and volatile solids

The total solids, ash content, and volatile solids of the feed and permeate samples before and after overnight fouling are presented in Table 4.3.

The initial feed contained 22.79% total solids, while the initial permeate contained 15.48%. A similar trend was observed for ash content, which decreased from 15.73% in the feed to 12.16% in the permeate. This shows that the permeate still contained a considerable amount of dissolved material and inorganic compounds, but at lower concentrations than the feed.

Table 4.3. Total solids, ash content, and volatile solids of feed and permeate samples.

Sample	Description	Total solids (%)	Ash (%)	Volatile solids (%)
1	Initial feed	22.79	15.73	7.05
2	Initial permeate	15.48	12.16	3.33
3	Feed after overnight fouling	24.29	17.52	6.77
4	Permeate after overnight fouling	17.34	13.49	3.85

The volatile solids content decreased from 7.05% in the initial feed to 3.33% in the initial permeate. Since volatile solids are associated with the organic fraction of the sample, this decrease suggests that part of the organic material was retained by the membrane during filtration. However, the presence of volatile solids in the permeate shows that smaller dissolved organic compounds still passed through the membrane.

After overnight fouling, the feed sample showed slightly higher total solids and ash content than the initial feed, increasing from 22.79% to 24.29% and from 15.73% to 17.52%, respectively. This may be related to concentration of the feed during long-term recirculation and permeate production. Since only a limited number of samples were analysed, these values should be interpreted as supporting information for the filtration behaviour rather than as a complete mass balance.

4.3.3 Lignin concentration

Lignin-related concentration was calculated from the absorbance measured at 280 nm using the dilution factor and the absorption coefficient reported for black liquor analysis. The calculated values are presented in Table 4.4.

The calculated lignin concentration was higher in the feed samples than in the permeate samples. This confirms that lignin-related compounds were partly retained by the ultrafiltration membrane. The initial feed contained approximately 133.1 g L^{-1} lignin-equivalent material, while the initial permeate contained approximately 41.6 g L^{-1}.

Table 4.4. UV–Vis absorbance and calculated lignin concentration of feed and permeate samples.

Sample	Description	Dilution factor	Absorbance at 280 nm	Calculated lignin concentration (g L^{-1})
1	Initial feed	4000	0.785	133.1
2	Initial permeate	1200	0.819	41.6
3	Feed after overnight fouling	5000	0.834	176.7
4	Permeate after overnight fouling	1200	0.833	42.4

After overnight fouling, the calculated feed concentration increased to 176.7 g L^{-1}. This increase may be related to concentration of the feed during long-term recirculation and permeate removal. In contrast, the permeate lignin concentration remained almost unchanged, increasing only slightly from 41.6 to 42.4 g L^{-1}. This suggests that the passage of lignin-related compounds through the membrane remained relatively stable during the overnight fouling experiment.

4.4 Membrane surface characterisation

Membrane surface characterisation was performed to compare the conditioned membrane, the fouled membrane after black liquor filtration, and the cleaned membrane after the validation cleaning experiment. SEM–EDS was used to examine surface morphology and elemental composition, AFM was used to evaluate surface topography and roughness, and BET nitrogen adsorption–desorption analysis was used to assess possible changes in surface area and pore-related properties.

4.4.1 SEM–EDS results

SEM analysis was used to compare the surface morphology of the conditioned, fouled, and cleaned membrane samples. The representative images in Figure 4.6. show clear differences between the three membrane states.

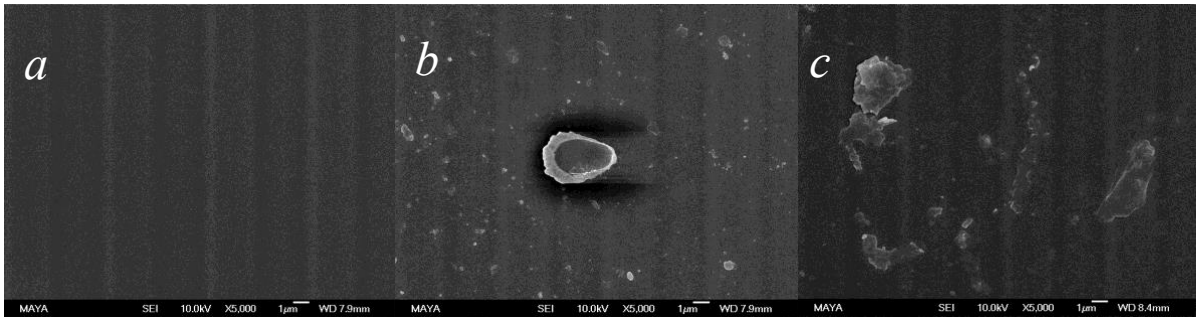

Figure 4.6. SEM images of (a) conditioned membrane, (b) fouled membrane, and (c) cleaned membrane after validation cleaning at ×5000 magnification.

The conditioned membrane surface appeared mostly smooth, although isolated particles were observed in some areas. Since these particles were present before black liquor filtration, they

were not interpreted as fouling deposits and may be related to sample handling, cutting, or surface contamination.

After black liquor filtration, the membrane surface became more heterogeneous. Local deposits and agglomerated structures were visible on the fouled membrane, indicating that the fouling layer was not evenly distributed over the surface. This non-uniform surface coverage is important because it suggests that fouling did not occur as a completely homogeneous layer, but rather as local accumulation of material on the membrane surface.

After chemical cleaning, the surface appeared cleaner than the fouled sample, although some irregularities and possible residual deposits were still visible. This suggests that the cleaning step removed part of the deposited material but did not completely restore the original membrane surface. This observation agrees with the flux recovery results, where cleaning improved the membrane performance but did not restore 100% of the initial pure water flux.

The residual deposits observed after cleaning are consistent with previous observations that alkaline cleaning does not remove all inorganic residues from kraft black liquor fouling layers [33, 34]. This may also explain why the flux recovery did not reach 100% after the validation cleaning.

EDS analysis was used to support the SEM observations by comparing the elemental composition of selected surface areas. The EDS spectra showed carbon and oxygen signals for all membrane samples. Gold (Au) and palladium (Pd) were also detected, but these signals originated from the sputter-coating layer applied during sample preparation and were therefore not interpreted as part of the membrane material or fouling layer.

For the conditioned membrane, the surface was mostly uniform, although isolated particles were observed in some areas. Since these particles were already present before black liquor filtration, they were not considered as fouling deposits. Their origin could not be confirmed from SEM–EDS alone, but they may be related to sample handling, cutting, storage, or local surface contamination.

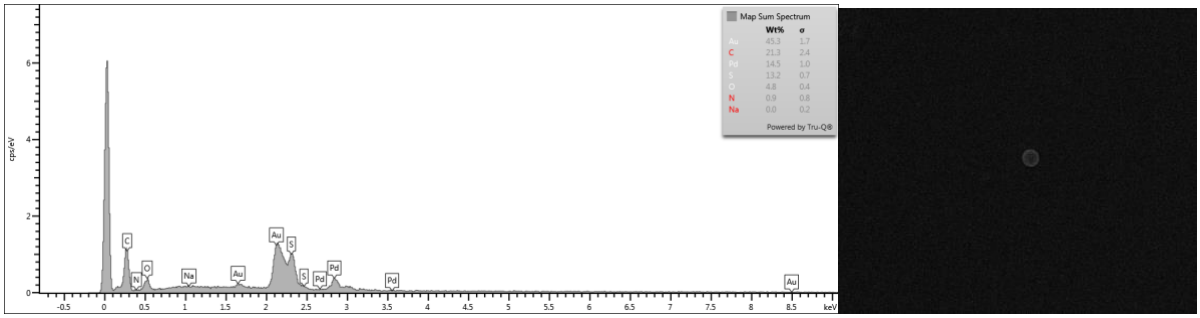

Figure 4.7. Representative EDS spectrum and selected SEM/EDS map of the conditioned membrane surface.

The fouled membrane showed a stronger carbon signal together with oxygen, sulphur, sodium, and nitrogen. Carbon and oxygen may originate from both the polymeric membrane material and deposited organic material. Sulphur can be associated with the polyethersulfone active layer as well as sulphur-containing inorganic species from black liquor, and therefore cannot be used alone as direct evidence of fouling. Sodium is more likely related to inorganic residues from

black liquor or alkaline solutions used during the experiment. The nitrogen signal may indicate nitrogen-containing residues or local contamination.

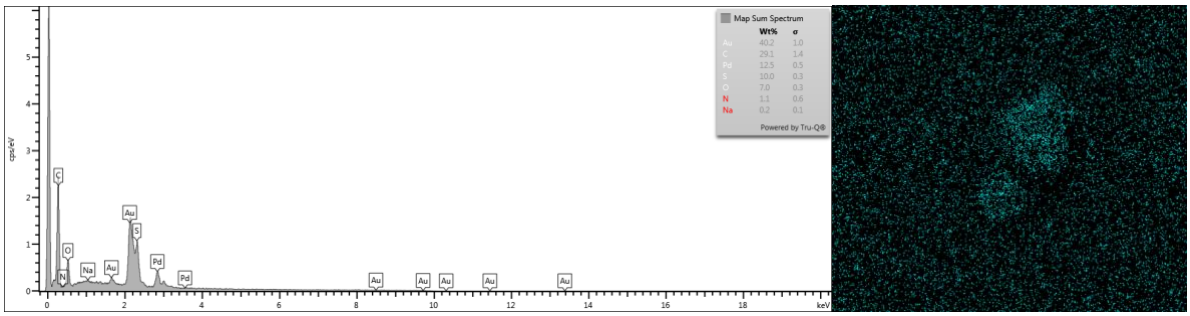

Figure 4.8. Representative EDS spectrum and carbon distribution map of the fouled membrane surface.

After cleaning, residual particles and carbon-containing surface features were still observed in some areas. This indicates that chemical cleaning reduced the visible fouling layer but did not completely remove all surface deposits. In one analysed area of the cleaned membrane, silicon and oxygen were detected in one analysed local particle. This particle may be related to inorganic contamination, silicate-containing material, or handling/laboratory contamination; however, its origin cannot be confirmed based only on the EDS spectrum.

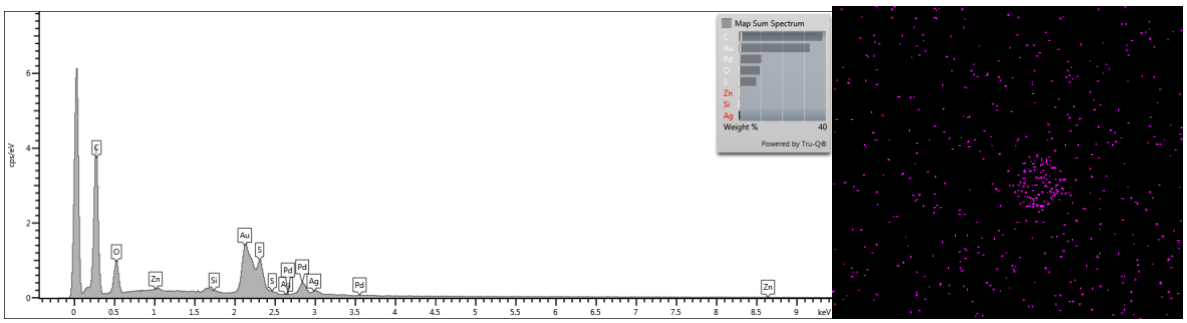

Figure 4.9. Representative EDS spectrum and selected particle map of the cleaned membrane surface.

4.4.2 AFM results

AFM analysis was performed to evaluate changes in membrane surface morphology before fouling, after fouling, and after cleaning. Representative 3D topography images are presented in Figure 4.10. The images were obtained from 5 × 5 µm scan areas.

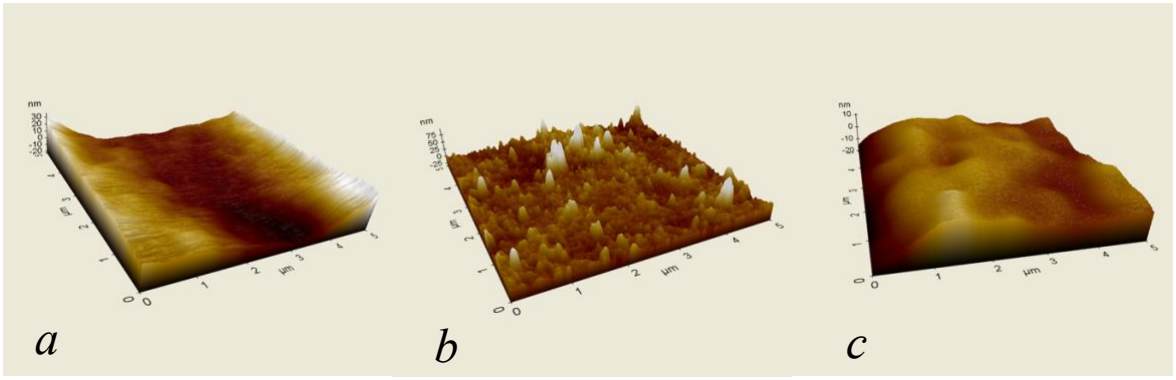

Figure 4.10. AFM 3D topography images of (a) conditioned membrane, (b) fouled membrane, and (c) cleaned membrane after validation cleaning. Scan size: 5 × 5 µm.

The conditioned membrane showed a relatively smooth surface with limited local height variations. After black liquor filtration, the AFM image showed a more heterogeneous surface with localized elevated structures, which agrees with the SEM observation of deposited material on the fouled surface. After cleaning, the surface appeared more uniform, indicating partial removal of deposits. However, remaining local irregularities show that the membrane surface was not fully restored to its initial condition.

Average roughness parameters are presented in Table 4.5. *Rq* represents the root mean square roughness, while *Ra* represents the arithmetic average roughness of the selected scan area. *Rpv* describes the peak-to-valley height difference and was included to show the local height range of the measured surface.

Table 4.5. AFM roughness parameters of conditioned, fouled, and cleaned membrane surfaces.

Membrane state	Mean Rq (nm)	Mean Ra (nm)	Mean Rpv (nm)
Conditioned	7.18	5.98	42.95
Fouled	5.24	3.68	64.58
Cleaned	3.63	2.83	27.13

In this study, *Ra* and *Rq* decreased after fouling, from 5.98 to 3.68 nm and from 7.18 to 5.24 nm, respectively. Therefore, the average roughness parameters did not indicate uniform roughening of the membrane surface. However, *Rpv* increased from 42.95 to 64.58 nm after fouling, showing that the fouled membrane contained stronger local height variations. For this reason, *Rpv* was the most informative roughness parameter for interpreting the AFM results in this study, because the fouling appeared to occur as localised deposits rather than as a uniform rough layer, in agreement with the AFM topography and SEM observations.

After cleaning, *Rq*, *Ra*, and *Rpv* decreased to 3.63, 2.83, and 27.13 nm, respectively. The decrease in *Rpv* from 64.58 to 27.13 nm suggests that chemical cleaning reduced the local elevated structures observed after fouling.

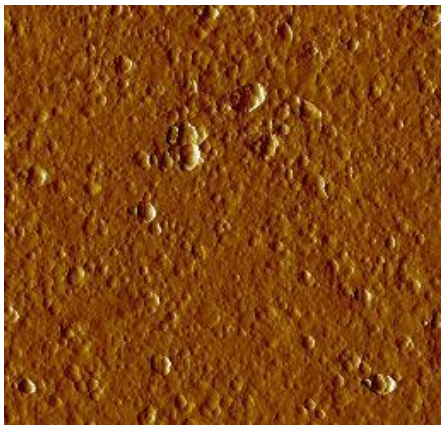

Figure 4.11. AFM amplitude image of the fouled membrane surface after black liquor filtration. Scan size: 5 × 5 µm.

The AFM amplitude image of the fouled membrane provides additional evidence of local surface heterogeneity after black liquor filtration. Some regions appeared relatively smooth, while other areas showed clustered deposited structures, which may indicate local variations in foulant accumulation. This observation is consistent with the SEM images that suggests that fouling did not form a uniform continuous layer over the membrane surface, but rather accumulated locally.

4.4.3 BET analysis

BET nitrogen adsorption–desorption analysis was used to evaluate whether fouling and cleaning caused measurable changes in the nitrogen-accessible surface area of the membrane samples. In addition to BET surface area, the instrument report provided BJH desorption pore parameters, including cumulative pore volume and average pore width. These values were used as supporting information to compare possible pore-related changes between the conditioned, fouled, and cleaned membranes. The obtained values are summarized in Table 4.6.

Table 4.6. BET and BJH parameters of conditioned, fouled, and cleaned membrane samples.

Parameter	Conditioned	Fouled	Cleaned
Surface area ($m^2\ g^{-1}$)	8.8814	8.7191	8.6764
BJH cumulative pore volume ($cm^3\ g^{-1}$)	0.0311	0.0355	0.0351
BJH desorption average pore width (Å)	161.8	175.2	168.2

The surface area changed only slightly between the three membrane states, decreasing from 8.88 $m^2\ g^{-1}$ for the conditioned membrane to 8.72 $m^2\ g^{-1}$ after fouling and 8.68 $m^2\ g^{-1}$ after cleaning. This indicates that black liquor filtration and subsequent cleaning did not cause a clear change in the overall nitrogen-accessible surface area. In contrast, the BJH cumulative pore volume increased from 0.0311 to 0.0355 $cm^3\ g^{-1}$ after fouling and remained close to this value after cleaning, at 0.0351 $cm^3\ g^{-1}$. The average pore width showed the same trend, increasing from 161.8 to 175.2 Å after fouling and decreasing slightly to 168.2 Å after cleaning. These changes suggest that fouling affected the pore-related parameters to a small extent, but the differences were limited and should not be interpreted as direct evidence of a specific fouling mechanism.

Similar changes in pore-related parameters after fouling of polymeric ultrafiltration membranes with wood-based streams were reported by Virtanen et al. [35], who observed an increase in cumulative pore volume after fouling that could identify the formation of a porous fouling layer. The same tendency was observed in the present work, although the magnitude of the change was smaller.

At the same time, the relatively small differences in BET surface area indicate that nitrogen adsorption did not capture a major overall structural change of the membrane. This is important when compared with the flux, SEM, and AFM results, where fouling was clearly visible through flux decline and localized surface deposits. Therefore, these BET results should be interpreted as complementary rather than direct evidence of the fouling mechanism. One possible explanation is that fouling occurred mainly as localized surface deposits or in structural regions that were not strongly reflected in the BET/BJH parameters. The complete nitrogen adsorption–desorption isotherms and BJH pore size distribution plots are provided in Appendix A.

5. Conclusion

This study investigated chemical cleaning of a polymeric ultrafiltration membrane used for black liquor filtration. The main objective was to evaluate how cleaning temperature, cleaning-agent concentration, and cleaning time affected membrane performance recovery after fouling. The fouling procedure was kept the same for all experiments; however, the fouling factor varied from 33.56% to 56.17%, showing that the initial fouling extent was not fully identical between membrane samples.

Flux recovery after cleaning varied from 53.63% to 75.36%. The highest measured flux recovery in the experimental design was obtained at 50 °C, 1 wt.% cleaning-agent concentration, and 30 min cleaning time. This experiment also had the lowest fouling factor, which means that its high recovery may have been partly influenced by the lower initial fouling extent. Therefore, flux recovery should be interpreted together with the fouling factor, rather than as an isolated cleaning-performance indicator.

A full factorial design was used as a screening approach to evaluate the influence of the three cleaning parameters on flux recovery. The statistical model indicated that cleaning temperature had the largest effect, followed by cleaning-agent concentration and cleaning time. However, none of the factors were statistically significant at the 95% confidence level, and the model had limited predictive accuracy. The prediction profiler suggested 50 °C, 1 wt.% cleaning-agent concentration, and 60 min cleaning time as the most favourable condition within the investigated range. This condition was therefore selected for the validation filtration experiment, even though the highest measured recovery in the original design was obtained after 30 min.

The validation experiment resulted in a flux recovery of 76.43%, compared with the model-predicted value of 68.42%. This value was higher than the highest recovery obtained in the original experimental set. However, the highest measured recovery in the original experimental design was obtained in the experiment with the lowest fouling factor, indicating that differences in the initial fouling extent may have influenced the apparent cleaning performance. The validation result supports the practical trend that cleaning at 50 °C and 1 wt.% cleaning-agent concentration improved flux recovery. However, the difference between 30 and 60 min was small, and cleaning time had the weakest effect in the model.

Membrane characterization supported the filtration results. SEM–EDS and AFM showed that black liquor filtration led to localized deposits and a more heterogeneous membrane surface, while chemical cleaning partly reduced these surface features. BET nitrogen adsorption–desorption analysis showed only minor changes in nitrogen-accessible surface area and pore-related parameters. This suggests that the main observable fouling effects were related mainly to surface deposits rather than large measurable changes in the overall pore structure. Overall, the results show that cleaning temperature and cleaning-agent concentration were more relevant than cleaning time for improving flux recovery under the tested conditions, but additional replicated experiments would be needed to confirm the trends and improve the reliability of the model.

6. Future Work

Future work should first include additional cleaning experiments with replicated runs. In this study, the fouling factor varied between membrane samples even though the same fouling procedure was applied. Repeating selected conditions, especially 50 °C with 1 wt.% cleaning-agent concentration at both 30 and 60 min, would help to confirm whether the longer cleaning time provides a real improvement or whether the difference is mainly caused by sample-to-sample variation.

Additional cleaning times, such as 45 and 90 min, could also be tested to determine whether the effect of time reaches a plateau. To improve the DOE model, intermediate factor levels should be added, for example 40 °C and 60 °C for temperature and 0.75 wt.%, or 1.5 wt.% for cleaning-agent concentration. These additional levels would make it possible to evaluate whether the observed trends are linear or whether an optimum exists within a narrower range.

Future experiments should also include ceramic membranes using the same black liquor fouling procedure and the same cleaning conditions as those used for the polymeric membrane. This would allow direct comparison between polymeric and ceramic membranes.

For membrane characterisation, future work should combine SEM–EDS and AFM with methods that give more direct information about chemical composition and active pore structure. FTIR spectroscopy could be used to identify functional groups from lignin-related organic material remaining on the membrane surface after fouling and cleaning. Contact angle measurements could show whether fouling or cleaning changed the surface hydrophilicity.

References

[1] Isikgor FH, Becer CR. Lignocellulosic biomass: a sustainable platform for the production of bio-based chemicals and polymers. Polymer Chemistry. 2015 Jan 1;6(25):4497–559. Available from: https://doi.org/10.1039/c5py00263j

[2] Li T, Takkellapati S. The current and emerging sources of technical lignins and their applications. Biofuels Bioproducts and Biorefining. 2018 Jul 10;12(5):756–87. Available from: https://doi.org/10.1002/bbb.1913

[3] Tran H, Vakkilainen EK. The kraft chemical recovery process. TAPPI Kraft Recovery Short Course; 2016.

[4] Gellerstedt G, Tomani P, Axegård P, Backlund B. Lignin Recovery and Lignin-Based Products. In: Integrated Forest Biorefineries: Challenges and Opportunities. 2012. p. 180–210. Available from: https://doi.org/10.1039/9781849735063-00180

[5] Zhu W. Precipitation of kraft lignin: yield and equilibrium. Doctoral thesis. Gothenburg: Chalmers University of Technology; 2015.

[6] Uloth VC, Wearing JT. Kraft lignin recovery: acid precipitation versus ultrafiltration, Part I: Laboratory test results. Pulp and Paper Canada. 1989; 90(9): 67–71.

[7] Wallberg O, Jönsson AS. Separation of lignin in kraft cooking liquor from a continuous digester by ultrafiltration at temperatures above 100°C. Desalination. 2006 Jul 30;195(1–3):187–200. Available from: https://doi.org/10.1016/j.desal.2005.11.011

[8] Wallberg O. Extraction of Lignin from Kraft Cooking Liquor by Ultrafiltration. Lund University Publications. 2005. Available from: https://lup.lub.lu.se/record/545518

[9] Humpert D, Ebrahimi M, Czermak P. Membrane Technology for the Recovery of Lignin: A review. Membranes. 2016 Sep 6;6(3):42. Available from: https://doi.org/10.3390/membranes6030042

[10] Battestini Vives M. Nanofiltration of kraft black liquor: Process development and techno-economic evaluation. Doctoral thesis. Lund University; 2024. ISBN 978-91-8096-062-5.

[11] Al-Amoudi A, Lovitt RW. Fouling strategies and the cleaning system of NF membranes and factors affecting cleaning efficiency. Journal of Membrane Science. 2007 Jul 31;303(1–2):4–28. Available from: https://doi.org/10.1016/j.memsci.2007.06.002

[12] Mulder M. Basic principles of membrane Technology. 1996. Available from: https://doi.org/10.1007/978-94-009-1766-8

[13] Cui ZF, Jiang Y, Field RW. Fundamentals of Pressure-Driven membrane Separation Processes. In: Membrane Technology. 2010. p. 1–18. Available from: https://doi.org/10.1016/b978-1-85617-632-3.00001-x

[14] Hunger K, Schmeling N, Jeazet HBT, Janiak C, Staudt C, Kleinermanns K. Investigation of Cross-Linked and Additive Containing Polymer Materials for Membranes with Improved Performance in Pervaporation and Gas Separation. Membranes. 2012 Oct 22;2(4):727–63. Available from: https://doi.org/10.3390/membranes2040727

[15] Van Der Bruggen B. Microfiltration, ultrafiltration, nanofiltration, reverse osmosis, and forward osmosis. In: Elsevier. 2018. p. 25–70. Available from: https://doi.org/10.1016/b978-0-12-813483-2.00002-2

[16] Battestini Vives M, Thuvander J, Arkell A, Lipnizki F. Pilot-scale nanofiltration and techno-economic evaluation of lignin recovery from kraft black liquor. Journal of Wood Chemistry and Technology. 2024 Nov 1;44(6):363–76. Available from: https://doi.org/10.1080/02773813.2024.2416651

[17] Field R. Fundamentals of fouling. Membrane Technology. 2010 Jan 27;1–23. Available from: https://doi.org/10.1002/9783527631407.ch1

[18] Field RW, Wu D, Howell JA, Gupta BB. Critical flux concept for microfiltration fouling. Journal of Membrane Science. 1995 Apr 1;100(3):259–72. Available from: https://doi.org/10.1016/0376-7388(94)00265-z

[19] Rudolph G. Investigations on membrane fouling and cleaning in ultrafiltration processes in lignocellulosic biorefineries. Lund University Publications (Lund University). 2021. Available from: https://lup.lub.lu.se/record/8633874e-e2d7-46a6-84e5-159b4af61c39

[20] Baker RW. Membrane Technology and Applications. 2004. Available from: https://doi.org/10.1002/0470020393

[21] Sjöström E. Wood chemistry: fundamentals and applications. 2nd ed. Academic Press; 1993.

[22] Tomani P. The LignoBoost process. Cellulose Chemistry and Technology. 2010; 44(1–3): 53–58.

[23] Arkell A, Olsson J, Wallberg O. Process performance in lignin separation from softwood black liquor by membrane filtration. Chemical Engineering Research and Design. 2014; 92(9): 1792–1800. doi:10.1016/j.cherd.2013.12.018

[24] Pola L, Collado S, Oulego P, Díaz M. Kraft black liquor as a renewable source of value-added chemicals. Chemical Engineering Journal. 2022 Jun 21;448:137728. Available from: https://doi.org/10.1016/j.cej.2022.137728

[25] Jönsson AS, Nordin AK, Wallberg O. Concentration and purification of lignin in hardwood kraft pulping liquor by ultrafiltration and nanofiltration. Chemical Engineering Research and Design. 2008 Aug 6;86(11):1271–80. Available from: https://doi.org/10.1016/j.cherd.2008.06.003

[26] Jönsson AS. Membranes for lignin and hemicellulose recovery in pulp mills. In: Elsevier. 2016. p. 105–33. Available from: https://doi.org/10.1016/b978-0-08-100451-7.00005-0

[27] Toledano A, García A, Mondragon I, Labidi J. Lignin separation and fractionation by ultrafiltration. Separation and Purification Technology. 2010 12;71(1):38–43. Available from: https://doi.org/10.1016/j.seppur.2009.10.024

[28] Sharma M, Alves P, Gando-Ferreira L. Lignin Recovery from Black Liquor Using Integrated UF/NF Processes and Economic Analysis. Membranes. 2023 Feb 16;13(2):237. Available from: https://doi.org/10.3390/membranes13020237

[29] Dafinov A, Font J, Garcia-Valls R. Processing of black liquors by UF/NF ceramic membranes. Desalination. 2005 Mar 1;173(1):83–90. Available from: https://doi.org/10.1016/j.desal.2004.07.044

[30] Alfa Laval AB. GR80PP flat sheet ultrafiltration membrane — product specification sheet. Sweden: Alfa Laval Corporate AB; 2020.

[31] Alfa Laval AB. TestUnit M20 — stand-alone pilot plant system. Alfa Laval Corporate AB. Available from: https://www.alfalaval.se/produkter/separering/membran/labstak/labstak-m20/

[32] Sluiter A, Hames B, Ruiz R, Scarlata C, Sluiter J, Templeton D. Determination of ash in biomass: laboratory analytical procedure (LAP). Golden (CO): National Renewable Energy Laboratory; 2008. Report No.: NREL/TP-510-42622.

[33] Battestini Vives M, Xiao X, Lipnizki F, Rudolph-Schöpping G. Response surface methodology to optimize membrane cleaning in nanofiltration of kraft black liquor. Separation and Purification Technology. 2024 Jun 29;354:128626. Available from: https://doi.org/10.1016/j.seppur.2024.128626

[34] Xiao X, Battestini Vives M, Lipnizki F, Rudolph-Schöpping G. Evaluation of the adsorptive behaviour of kraft black liquor on nanofiltration model membrane surfaces via quartz crystal microbalance with dissipation monitoring (QCM-D). Journal of Membrane Science. 2025 Mar 26;725:124043. Available from: https://doi.org/10.1016/j.memsci.2025.124043

[35] Virtanen T, Rudolph G, Lopatina A, Al-Rudainy B, Schagerlöf H, Puro L, et al. Analysis of membrane fouling by Brunauer-Emmett-Teller nitrogen adsorption/desorption technique. Scientific Reports. 2020 Feb 25;10(1):3427. Available from: https://doi.org/10.1038/s41598-020-59994-1

Appendix A

BET nitrogen adsorption–desorption isotherms

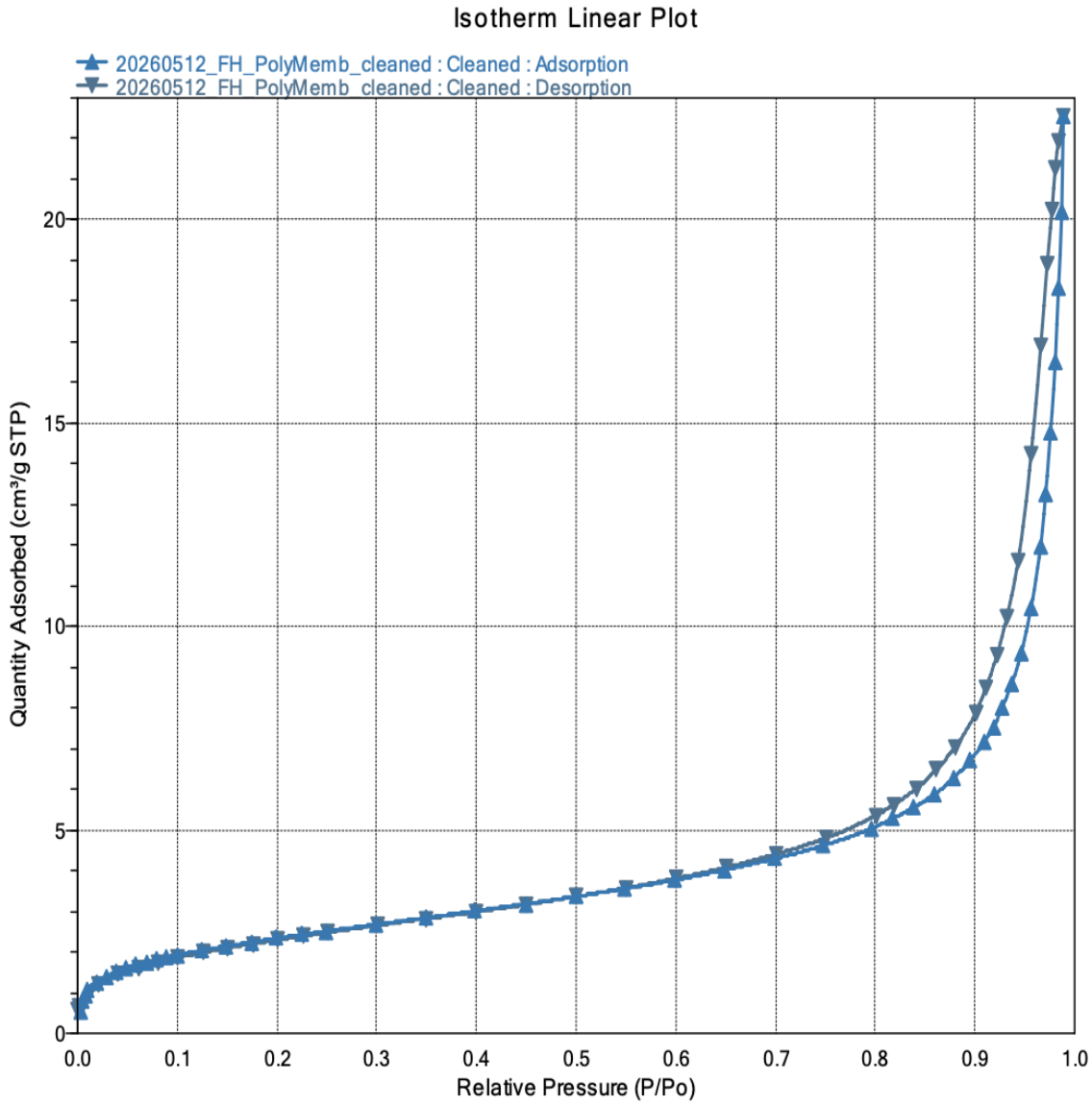

Figure A.1. Nitrogen adsorption–desorption isotherm of the cleaned membrane sample.

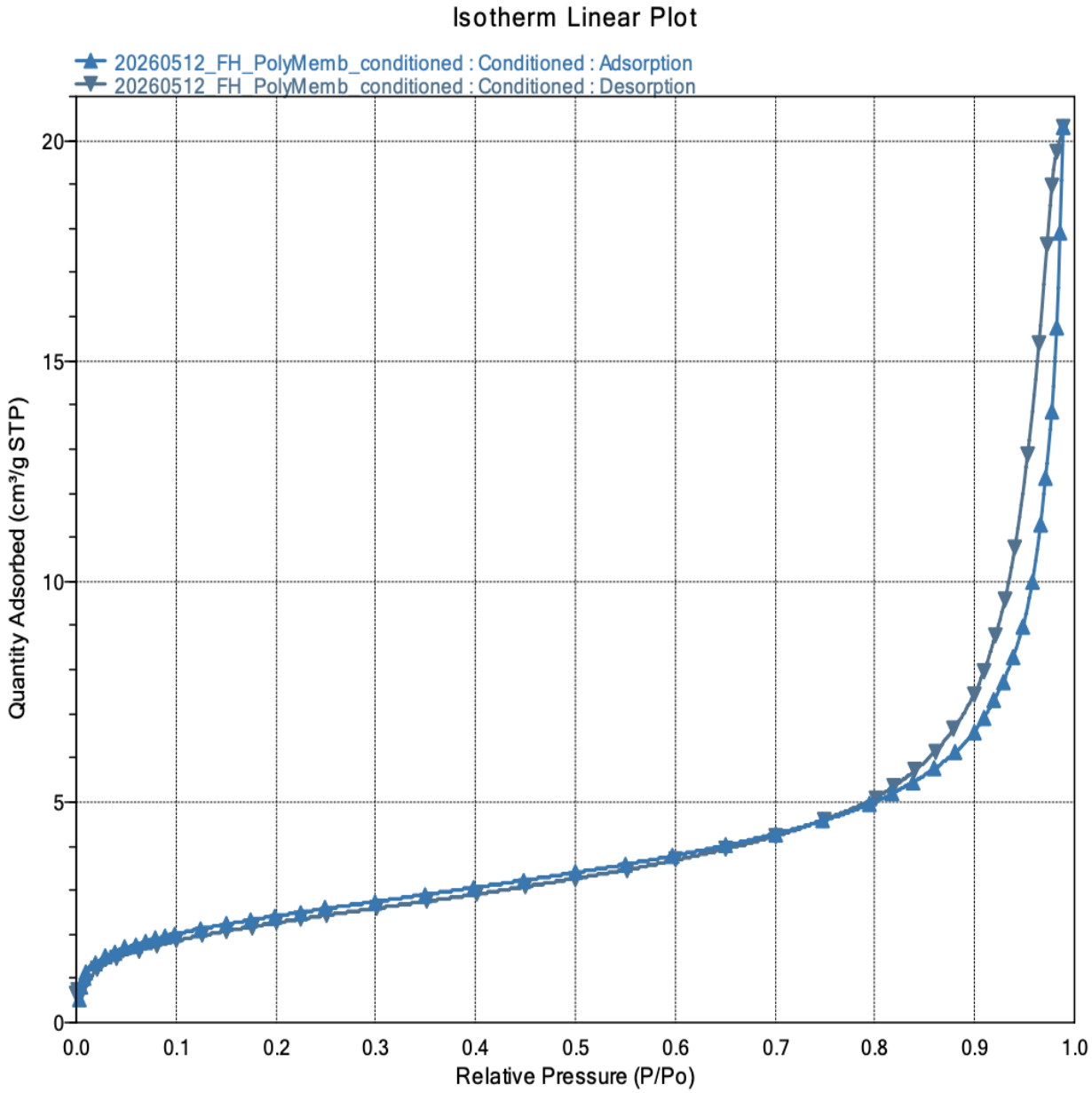

Figure A.2. Nitrogen adsorption–desorption isotherm of the conditioned membrane sample.

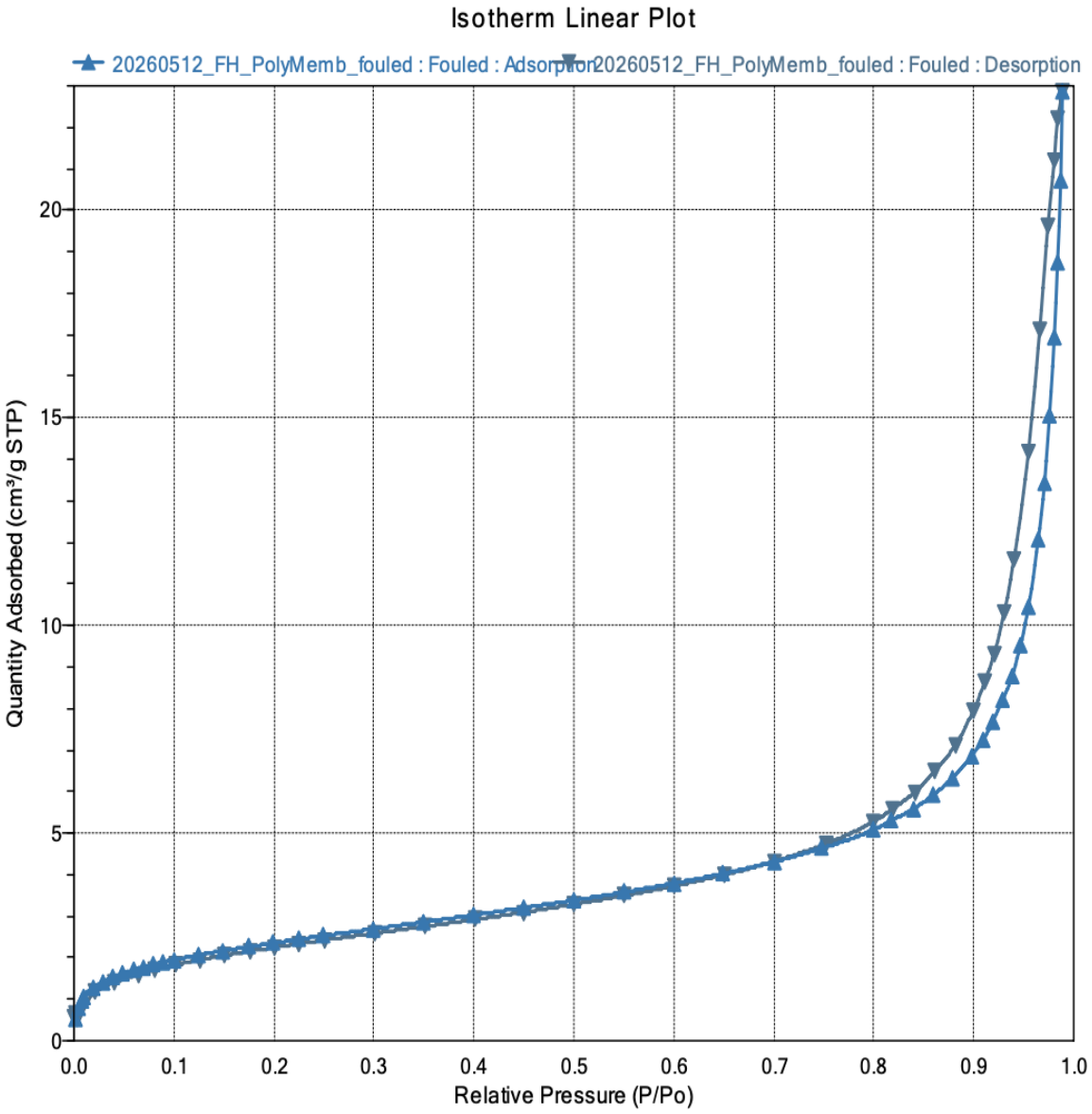

Figure A.3. Nitrogen adsorption–desorption isotherm of the fouled membrane sample.